reflux for 30 h. The reaction mixture was analyzed by GLC as being 1-[diethyl(3,5-dimethylbenzyl)silyl]-2-(diethylsilyl)benzene (9) (28% yield) and unchanged 1 (3% yield). Pure 9 was isolated by preparative GLC: MS m/e 368 (M^+); IR 2955, 2874, 2146, 1602, 1457, 1417, 1117, 1016, 809 cm^{-1}; ^1H NMR 0.81–1.05 (m, 20H, EtSi), 2.18 (s, 6H, two Me), 2.40 (s, 2H, CH_2), 4.65 (quint, 1H, HSi, J = 3.3 Hz), 6.56 (broad s, 2H, mesityl ring protons), 6.67 (broad s, 1H, mesityl ring proton), 7.25–7.57 (m, 4H, phenylene ring protons); ^{13}C NMR 4.69 (two carbons), 7.51, 8.41 (EtSi), 21.26 (Me), 23.18 (CH_2), 125.64, 126.41, 127.69, 127.81, 135.04, 135.67, 137.30, 139.94, 142.71, 143.75 (mesityl and phenylene ring carbons); ^{29}Si NMR −9.69, 1.00. Anal. Calcd for $C_{23}H_{36}Si_2$: C, 74.92; H, 9.84. Found: C, 74.91; H, 9.81.

Reaction of 1 with Hexane. A mixture of 0.4229 g (1.70 mmol) of 1 and 46 mg (8.66×10^{-2} mmol) of tetrakis(triethylphosphine)nickel(0) in 0.6 mL of dry hexane was heated in a degassed sealed tube at 150 °C for 24 h. GLC analysis of the mixture showed the presence of 8% of the starting compound 1 and a small amount of an unidentified product (less than 4% yield). Nonvolatile products were isolated by precipitation of the mixture from methanol–chloroform: IR 3050, 2954, 2153 (H–Si), 1462, 1455, 1416, 1378, 1348, 1233, 1138, 1010, 972, 800, 704 cm^{-1}; ^1H NMR 0.45–1.12 (m, EtSi), 4.21 (broad s, HSi), 7.31–7.72 (m, phenylene ring protons).

Reaction of 1 with a 1:1 Mixture of Benzene and Toluene. A mixture of 0.6829 g (2.75 mmol) of 1 and 74 mg (1.39×10^{-1} mmol) of tetrakis(triethylphosphine)nickel(0) in the mixed solvent consisting of 5.63 g (72 mmol) of benzene and 6.63 g (72 mmol) of toluene was heated to reflux for 5 h. The mixture was analyzed by GLC as being **4a** (56% yield), **5a** (22% yield), and **5b** (9% yield). All spectral data obtained for **4a**, **5a**, and **5b** were identical with those of authentic samples.

Reaction of 1 with a 1:1 Mixture of Benzene and Mesitylene. A mixture of 0.5310 g (2.14 mmol) of 1 and 55 mg (1.04×10^{-1} mmol) of the nickel catalyst in the mixed solvent consisting of 5.80 g (74 mmol) of benzene and 8.85 g (74 mmol) of mesitylene was heated to reflux for 5 h. GLC analysis of the reaction mixture showed the presence of **4a** (69% yield) as the sole product. All spectral data for **4a** were identical with those of an authentic sample.

Acknowledgment. This research was supported in part by a Grant-in-Aid for Scientific Research on the Priority Area of Organic Unusual Valency, No. 03233105, from the Ministry of Education, Science, and Culture. We thank Professor A. Nakamura, Department of Macromolecular Science, Faculty of Science, Osaka University, and Professor S. Murahashi, Department of Chemistry, Faculty of Engineering Science, Osaka University, for useful discussion. We also express our appreciation to Shin-Etsu Chemical Co. Ltd., Nitto Electric Industrial Co. Ltd., Dow Corning Japan Ltd., and Toshiba Silicone Co. Ltd. for financial support.

OM920232+

Heterobimetallic Complexes Containing Methylaminobis(difluorophosphine)

Joel T. Mague* and Zhaiwei Lin

Department of Chemistry, Tulane University, New Orleans, Louisiana 70118

Received July 17, 1992

The use of $cpFeCl(PNP)_2$ and $Mo(CO)_3(PNP)_2$ (cp = cyclopentadienyl; PNP = $MeN(PF_2)_2$) as precursors to heterobimetallic complexes is reported. The former generally reacts via chloride transfer to low-valent metal complexes while the latter either gives heterobimetallic complexes bridged by two PNP ligands or acts as a source of PNP ligands. $cpFeCl(PNP)_2$ with $Co_2(CO)_8$ gives $CoCl_2$ and $cpFe(\mu\text{-}PNP)_2Co(CO)_2$ (1) and with $Pt(C_2Ph_2)(PPh_3)_2$ forms $PtCl(PPh_3)(\mu\text{-}PF_2)(\mu\text{-}PF_2NMe)Fe(PF_2NHMe)cp$ (2) and $PtCl(P(O)F_2)(PPh_3)_2$ (7). The last is also formed from PNP and $PtCl_2(PPh_3)_2$. $Mo(CO)_3(PNP)_2$ with $Ni(CO)_2(PPh_3)_2$ or $Pt(C_2H_4)(PPh_3)_2$ gives $Mo(CO)_3(\mu\text{-}PNP)_2M(PPh_3)$ (M = Ni (3), Pt (4)) while with $MCl(CO)(PPh_3)_2$ the products are $Mo(CO)_3(\mu\text{-}PNP)_2IrCl(CO)(PPh_3)$ (M = Ir, 5) and $Mo(CO)_3(\mu\text{-}PNP)_2RhCl(PPh_3)$ (M = Rh, 6). Direct reaction of PNP with $Pt(C_2H_4)(PPh_3)_2$ and $cp_2Mo_2(CO)_4$ yields $Pt_2(\mu\text{-}PNP)_3(PPh_3)$ (8) and $cp_2Mo_2(CO)_4(\mu\text{-}PNP)$ (9), respectively. The ^{31}P NMR spectra of the complexes and related chemistry are discussed. The crystal structures of 1, 2, 4, 7, and 8 have been determined by X-ray crystallography. 1: monoclinic; $P2_1/n$; a = 8.750 (1), b = 19.908 (2), c = 10.719 (2) Å; β = 95.97 (1)°; Z = 4. 2: monoclinic; $P2_1/c$; a = 12.696 (2), b = 13.479 (2), c = 21.031 (1) Å; β = 92.620 (7)°; Z = 4. 4: orthorhombic; $Pbca$; a = 14.544 (1), b = 23.023 (1), c = 19.453 (2) Å; Z = 8. 7: monoclinic; $P2_1/c$; a = 11.828 (2), b = 20.678 (4), c = 8.317 (1) Å; β = 95.04 (1)°; Z = 2. 8: monoclinic; $P2_1/c$; a = 11.696 (2), b = 16.492 (2), c = 17.809 (2) Å; β = 103.465 (2)°; Z = 4.

Introduction

We have for a number of years been interested in the chemistry of bi- and trimetallic complexes stabilized by "short bite" phosphorus ligands such as $H_2C(PPh_2)_2$-(DPPM)[1] and $HC(PMe_2)_3$(tmpm).[2] The steric bulk of DPPM is such that access to the metal atoms in its bimetallic complexes is frequently quite restricted thus limiting the range of molecules which could be studied as substrates for bimetallic activation. We therefore sought less bulky ligands which could be expected to show a similar preference for bridging two metals, as opposed to forming monometallic chelates, thereby making the metal atoms accessible to a wider variety of potential substrates. An attractive class of ligands is that of formula $RN(PX_2)_2$ (R = alkyl; X = alkoxy, F).[3] Prior to our earlier work in

(1) (a) Mague, J. T. *Organometallics* **1986**, *5*, 918 and references therein. (b) Mague, J. T. *Polyhedron* **1990**, *9*, 2635. (c) Mague, J. T. *Polyhedron* **1992**, *11*, 677.

(2) Mague, J. T.; Lloyd, C. L. *Organometallics* **1992**, *11*, 26.

(3) (a) Brown, G. M.; Finholt, J. E.; King, R. B.; Bibber, J. W. *Inorg. Chem.* **1982**, *21*, 2139. (b) Mague, J. T.; Johnson, M. P. *Organometallics* **1990**, *9*, 1254. (c) Nixon, J. F. *J. Chem. Soc. A* **1973**, 2689.

0276-7333/92/2311-4139$03.00/0

this area, few complexes of these ligands with the platinum metals had been reported[4] and, to the best of our knowledge, no examples of heterobimetallic complexes were known. Following studies on complexes of $MeN(P(OR)_2)_2$ (R = Me, *i*-Pr) which provided examples of heterobimetallic complexes as well as some unusual binuclear tungsten complexes,[3b,5] we turned our attention to further chemistry of $MeN(PF_2)_2$ (PNP) which has previously provided a number of complexes with unusual structures.[6] The reported complexes $cpFeCl(\eta^1\text{-}MeN(PF_2)_2)_2$[7] (cp = cyclopentadienyl) and *fac*-$Mo(CO)_3(\eta^2\text{-}MeN(PF_2)_2)(\eta^1\text{-}MeN(PF_2)_2)$[6c] appear particularly suited for the formation of heterobimetallic complexes. This has been demonstrated for the former,[8] and we now report on further studies in this area.

Experimental Section

Materials and Measurements. All reactions were carried out under an atmosphere of prepurified nitrogen unless otherwise specified using standard Schlenk techniques. Solvents were purified by established methods and were distilled under nitrogen prior to use. Literature methods were used to prepare $MeN(PF_2)_2$,[7] $cpFeCl(MeN(PF_2)_2)_2$,[7] $Mo(CO)_3(MeN(PF_2)_2)_2$,[6c] $PtCl_2(PPh_3)_2$,[9] $Pt(C_2H_4)(PPh_3)_2$,[10] $Pt(C_2Ph_2)(PPh_3)_2$,[11] $(RhCl(COD))_2$ (COD = cycloocta-1,5-diene),[12] $IrCl(CO)(PPh_3)_2$,[13] $PtCl_2(NCPh)_2$,[14] and $cp_2Mo_2(CO)_4$.[15] Other organometallic starting materials were purchased from Strem chemicals. ^1H and $^{31}P\{^1H\}$ NMR spectra were obtained on an IBM-Bruker AF-200 spectrometer at 200.132 and 81.015 MHz, respectively, at ambient probe temperature unless otherwise noted. Proton and phosphorus chemical shifts are respectively referred to external tetramethylsilane (δ 0.0) and 85% H_3PO_4 (δ 0.0) with positive shifts downfield of the reference. Infrared spectra were obtained on a Mattson-Cygnus 100 Fourier transform spectrometer. All chromatographic separations were performed on 1.7 × 20-cm Florisil columns prepared in hexane under nitrogen. Microanalyses were performed by Galbraith Laboratories, Knoxville, TN.

$(\eta^5\text{-}C_5H_5)Fe(\mu\text{-}CH_3N(PF_2)_2)_2Co(CO)_2$ (1). A solution of 0.11 g (0.32 mmol) of $Co_2(CO)_8$ in 5 mL of hexane was added to 0.30 g (0.61 mmol) of $cpFeCl(MeN(PF_2)_2)_2$ in 10 mL of toluene at 0 °C whereupon vigorous gas evolution occurred and a blue solid precipitated. Filtration and evaporation of the filtrate under reduced pressure afforded the crude product as a purple powder. This was taken up in hexane and chromatographed. Elution with hexane gave a single purple band which was evaporated to dryness under reduced pressure to give 0.30 g (51%) of dark red-purple microcrystals, mp 85–87 °C. IR (hexane solution): 2024 (s), 1968 (s)[16] cm^{-1} (ν_{CO}). ^1H NMR (C_6D_6): δ 4.19 (s, 5 H, C_5H_5), 2.39 (br, 6 H, NCH_3).[17] $^{31}P\{^1H\}$ NMR (C_6D_6): δ (P_{Fe}) 192.5 (tm), δ (P_{Co}) 165.3 (m). Anal. Calcd for $C_9H_{11}P_4O_2N_2F_8FeCo$: C, 18.97; H, 1.94; N, 4.91. Found: C, 19.5; H, 1.8; N, 4.8.

$Pt(P(C_6H_5)_3)Cl(\mu\text{-}PF_2)(\mu\text{-}N(CH_3)PF_2)Fe(\eta^5\text{-}C_5H_5)\text{-}(PF_2NHCH_3)\cdot 0.7CH_2Cl_2$ (2). To 0.300 g (0.612 mmol) of $cpFeCl(MeN(PF_2)_2)_2$ in 7 mL of toluene was added dropwise a solution of 0.544 g (0.612 mmol) of $Pt(C_2Ph_2)(PPh_3)_2$ in 7 mL of toluene. The red-brown solution was stirred at room temperature for 20 h, and the solvent was then evaporated under reduced pressure. The resulting brown oil was taken up in 2 mL of dichloromethane and chromatographed. After the column was washed with hexane, it was eluted successively with dichloromethane and dichloromethane/acetone (1:1, v/v) which removed a broad orange band. The eluate was concentrated to ca. 2 mL and rechromatographed under the same conditions. The yellow eluate was taken to dryness under reduced pressure to afford a yellow powder which was finally recrystallized from a concentrated solution in dichloromethane/hexane at −5 °C, to afford amber crystals in ca. 20% yield. IR: 3295 (m) cm^{-1} (ν_{N-H}). ^1H NMR (C_6D_6): δ 7.86 (m), 7.03 (m), (15 H, C_6H_6), 4.27 (s, 1.4 H, CH_2Cl_2), 4.14 (s, 5 H, C_5H_5), 3.65 (d (J = 15.2 Hz), 3 H, PF_2NCH_3), 2.35 (dd (J = 10.6, 5.6 Hz), 3 H, PF_2NHCH_3). $^{31}P\{^1H\}$ NMR (C_6D_6): δ (PPh_3) 12.8 (m, $^1J_{Pt-P}$ = 3534 Hz), δ (PF_2NHCH_3) 193 (tddt, $^1J_{P-F}$ = 1105, $^2J_{P-P}$ = 132.0, 82.6 Hz), δ (PF_2NMe) 226.4 (tm, $^1J_{P-F}$ = 1160 Hz), δ (PF_2) 290.0 (tdd, $^1J_{Pt-P}$ = 3732, $^1J_{P-P}$ = 1142 Hz). Anal. Calcd for $C_{25.7}H_{28.4}P_4F_6N_2Cl_{2.4}FePt$: C, 32.86; H, 3.05. Found: C, 32.8; H, 3.4.

$Mo(CO)_3(\mu\text{-}CH_3N(PF_2)_2)_2Ni(P(C_6H_5)_3)$ (3). To 0.40 g (0.78 mmol) of $Mo(CO)_3(MeN(PF_2)_2)_2$ in 7 mL of toluene was added 0.50 g (0.78 mmol) of solid $Ni(CO)_2(PPh_3)_2$. The resulting suspension was stirred at room temperature for 10 h by which time a clear yellow solution had formed. The solvent was removed under reduced pressure and the yellow residue crystallized from dichloromethane/hexane (0.40 g, 67%), mp 175 °C dec. IR (CH_2Cl_2 solution): 2022 (s), 1968 (s), 1921 (m) cm^{-1} (ν_{CO}). ^1H NMR ($CDCl_3$): δ 7.34 (m, 15 H, C_6H_5), 2.90 (bt, 6 H, NCH_3). $^{31}P\{^1H\}$ NMR ($CDCl_3$): δ (PPh_3) 37.8 (t, $^2J_{P-P}$ = 33.7 Hz), δ (PNP) complex multiplet centered at 160.1. Anal. Calcd for $C_{23}H_{21}P_5O_4N_2F_8MoNi$: C, 33.08; H, 2.54; N, 3.36. Found: C, 34.0; H, 2.6; N, 3.1.

$Mo(CO)_3(\mu\text{-}CH_3N(PF_2)_2)_2Pt(P(C_6H_5)_3)$ (4). To 0.30 g (0.58 mmol) of $Mo(CO)_3(MeN(PF_2)_2)_2$ in 5 mL of toluene was added 0.44 g (0.59 mmol) of $Pt(C_2H_4(PPh_3)_2$ whereupon the solution turned yellow. Upon stirring at room temperature for 12 h an orange solution was obtained. This was filtered and the solvent removed in vacuo. The residue was recrystallized from dichloromethane/hexane at −5 °C to give a small quantity of powdery, yellow-orange flakes (yield ca. 30%). Satisfactory analytical data could not be obtained (see Discussion). IR (CH_2Cl_2 solution): 2013 (m), 1929 (s), 1894 (s) cm^{-1} (ν_{CO}). ^1H NMR ($CDCl_3$): δ 7.42 (m, 15 H, C_6H_5), 2.75 (br, 6 H, NCH_3). $^{31}P\{^1H\}$ NMR (CH_2Cl_2/acetone-d_6 202 K): δ (P_{Mo}) 172.0 (tm), δ (P_{Pt}) 174.0 (tm, $^1J_{Pt-P}$ = 6023 Hz), δ (PPh_3) 31.4 (br, $^1J_{Pt-P}$ = 2980 Hz).

$Mo(CO)_3(\mu\text{-}CH_3N(PF_2)_2)_2IrCl(CO)(P(C_6H_5)_3)$ (5). To a solution of 0.186 g (0.362 mmol) of $Mo(CO)_3(MeN(PF_2)_2)_2$ in 5 mL of toluene was added 0.25 g (0.36 mmol) of solid $IrCl(CO)(PPh_3)_2$. The cloudy suspension was stirred at room temperature for several minutes by which time the solid had dissolved to give an orange yellow solution. The solvent was removed in vacuo and the residue crystallized from dichloromethane/hexane (yield 0.4 g, 63%). IR (CH_2Cl_2 solution): 2037 (s), 1989 (vs), 1934 (s), 1889 (s) cm^{-1} (ν_{CO}). ^1H NMR ($CDCl_3$): δ 7.46 (m), 7.23 (m, 15 *H*, C_6H_5), 2.82 (br, 6 H, NCH_3). $^{31}P\{^1H\}$ NMR ($CDCl_3$): δ (PPh_3) 2.70 (t), δ (P_{Ir}) 101.0 (tm), δ (P_{Mo}) 163.3 (tm). Anal. Calcd for $C_{24}H_{21}P_5F_8N_2O_4ClMoIr$: C, 27.93; H, 2.06; N, 2.72. Found: C, 27.9; H, 2.2; N, 2.6.

$Mo(CO)_3(\mu\text{-}CH_3N(PF_2)_2)_2RhCl(P(C_6H_5)_3)\cdot 2CH_2Cl_2$ (6). To a solution of $RhCl(CO)(PPh_3)_2$ (0.26 g, 0.38 mmol) in 45 mL of

(4) (a) Field, J. S.; Haines, R. J.; Minshall, E.; Sampson, C. N.; Sundermayer, J.; Woollam, S. F.; Allen, C. C.; Boyens, J. C. A. *J. Chem. Soc., Dalton Trans.* **1991**, 2761 and references therein. (b) Haines, R. J.; Laing, M.; Meintjies, E.; Sommerville, P. *J. Organomet. Chem.* **1981**, *215*, C17. (c) Haines, R. J.; Meintjies, E.; Laing, M.; Sommerville, P. *J. Organomet. Chem.* **1981**, *216*, C19. (d) Field, J. S.; Haines, R. J.; Meintjies, E.; Sigwarth, B.; Van Rooyen, P. H. *J. Organomet. Chem.* **1984**, *268*, C43. (e) Haines, R. J.; Meintjies, E.; Laing, M. *Inorg. Chim. Acta* **1979**, *36*, L403. (f) Dulebohn, J. I.; Ward, D. L.; Nocera, D. G. *J. Am. Chem. Soc.* **1990**, *112*, 2969.

(5) Magee, J. T.; Johnson, M. P. *Organometallics* **1991**, *10*, 349.

(6) (a) Magee, J. T.; Johnson, M. P.; Lloyd, C. L. *J. Am. Chem. Soc.* **1989**, *111*, 5012. (b) Magee, J. T.; Johnson, M. P. *Acta Crystallogr.* **1990**, *C46*, 129. (c) King, R. B.; Shimura, M.; Brown, G. M. *Inorg. Chem.* **1984**, *23*, 1398. (d) Newton, M. G.; King, R. B.; Chang, M.; Pantaleo, N. S.; Gimeno, J. *J. Chem. Soc., Chem. Commun.* **1977**, 531. (e) Newton, M. G.; King, R. B.; Lee, T. W.; Norskov-Lauritzen, L.; Kumar, V. *J. Chem. Soc., Chem. Commun.* **1982**, 201.

(7) King, R. B.; Gimeno, J. *Inorg. Chem.* **1978**, *17*, 2390.

(8) Magee, J. T. *Organometallics* **1991**, *10*, 513.

(9) Bailar, J. C., Jr.; Itatani, H. *Inorg. Chem.* **1965**, *4*, 1618.

(10) Nagel, U. *Chem. Ber.* **1982**, *115*, 1998.

(11) Blake, D. M.; Roundhill, D. M. *Inorg. Synth.* **1978**, *18*, 122.

(12) Magee, J. T.; Lloyd, C. L. *Organometallics* **1988**, *7*, 983.

(13) Burk, M. J.; Crabtree, R. H. *Inorg. Chem.* **1986**, *25*, 931.

(14) Braunstein, P.; Bender, R.; Jud, J. *Inorg. Synth.* **1989**, *26*, 345.

(15) Curtis, M. D.; Nicephoros, A. F.; Messerle, L.; Sattelberger, A. P. *Inorg. Chem.* **1983**, *22*, 1559.

(16) Key to infrared band intensities: vs, very strong; s, strong; m, medium; w, weak.

(17) Key to NMR peak multiplicities: s, singlet; d, doublet; dd, doublet of doublets; t, triplet; dt, doublet of triplets; bt, broad triplet; tt, triplet of triplets; tdd, triplet of doublets of doublets; tddt, triplet of doublets of doublets of triplets; m, multiplet; tm, triplet of multiplets; br, broad.

Table I. Crystallographic Data for Complexes

	1	2	4	7	8
formula	$C_9H_{11}P_4F_8N_2O_2FeCo$	$C_{25.7}H_{28.4}P_4F_6N_2Cl_{2.4}FePt$	$C_{23}H_{21}P_5F_8N_2O_3MoPt$	$C_{37}H_{32}P_3F_2OCl_3Pt$	$C_{21}H_{24}P_7F_{12}N_3Pt_2$
fw, amu	569.96	879.78	971.32	925.03	1153.42
cryst syst	monoclinic	monoclinic	orthorhombic	monoclinic	monoclinic
sp gp	$P2_1/n$	$P2_1/c$	$Pbca$	$P2_1/c$	$P2_1/c$
a, Å	8.750 (1)	12.696 (2)	14.544 (1)	11.828 (2)	11.696 (2)
b, Å	19.908 (2)	13.479 (2)	23.023 (1)	20.678 (4)	16.492 (2)
c, Å	10.719 (2)	21.031 (1)	19.453 (2)	8.317 (1)	17.809 (2)
β, deg	95.97 (1)	92.620 (7)		95.04 (1)	103.465 (2)
V, Å^3	1857.0 (8)	3595 (1)	6514 (2)	2026 (1)	3342 (1)
Z	4	4	8	2	4
d_{calc}, g-cm^{-3}	2.04	1.62	1.98	1.52	2.29
μ, cm^{-1}	20.9	46.3	50.3	38.5	88.7
range trans factors	0.865–1.000	0.743–1.000	0.540–1.186	0.553–1.000	0.862–1.000
2θ range, deg	3.0–50.0	3.0–50.0	3.0–50.0	3.0–52.0	3.0–52.0
scan speed, deg of min^{-1}	0.9–8.2	1.3–16.4	0.8–4.1	1.3–16.4	1.3–16.4
no. of data collected	3608	6953	6331	4304	6408
cutoff for obsd data	$I \geq 2\sigma(I)$	$I \geq 3\sigma(I)$	$I \geq 2\sigma(I)$	$I \geq 3\sigma(I)$	$I \geq 3\sigma(I)$
no. of unique obsd data	1952	4522	2970	2741	4358
no of variables	244	361	388	236	406
R^a	0.031	0.034	0.054	0.043	0.025
$R_w{}^b$	0.036	0.055	0.057	0.074	0.034
GOF^c	1.07	1.80	1.53	2.72	1.15

$^a R = \sum||F_o| - |F_c||/\sum|F_o|$. $^b R_w = [\sum w(|F_o| - |F_c|)^2/\sum w(|F_o|)^2]^{1/2}$ with $w = 1/(\sigma_F)^2$; $\sigma_F = \sigma(F^2)/2F$; $\sigma(F^2) = [(\sigma_I)^2 + (0.04F^2)^2]^{1/2}$. ^{c}GOF = $[\sum w(|F_o| - |F_c|)^2/(N_o - N_v)]^{1/2}$ where N_o and N_v are, respectively, the number of observations and variables.

toluene/CH_2Cl_2 (5:4 v/v) was added 0.20 g (0.39 mmol) of $Mo(CO)_3(MeN(PF_2)_2)_2$. After 2 h the cloudy mixture had become a clear orange solution. Stirring was continued at room temperature overnight after which time the solvent was removed in vacuo and the crude product was taken up in 30 mL of toluene/CH_2Cl_2 (1:2 v/v) and filtered. Concentration of the filtrate in vacuo and dilution with hexane afforded the product as an orange powder in 74% yield (mp 220–230 °C). The analytical sample was recrystallized from a dichloromethane/hexane solution by slow evaporation in a stream of nitrogen and obtained as bright orange prisms. IR (Nujol mull): 1955 (s), 1904 (m), 1873 (s) cm^{-1} (ν_{CO}). ^{1}H NMR (C_6D_6): δ 7.58 (m), 7.08 (m, 15 H, C_6H_6), 2.17 (m, 6 H, NCH_3). $^{31}P\{^1H\}$ NMR (CH_2Cl_2/acetone-d_6, 248 K): δ (P_{Mo}) 167.7 (m), δ (P_{Rh}) 142.2 (m), 129.8 (m), δ (PPh_3) 15.0 (br). Anal. Calcd for $C_{25}H_{25}P_5F_8N_2O_3Cl_5RhMo$: C, 27.68; H, 2.33; N, 2.58. Found: C, 26.9; H, 2.2; N, 2.6.

$PtCl(P(O)F_2)(P(C_6H_5)_3)_2 \cdot CH_2Cl_2$ (7). To a filtered solution of 0.30 g (0.38 mmol) of $PtCl_2(PPh_3)_2$ in 10 mL of dichloromethane was added 0.07 g (0.41 mmol) of $MeN(PF_2)_2$. The solution was stirred at room temperature for 8 h during which time it had become cloudy. Following filtration through a pad of diatomaceous earth the colorless solution was diluted with diethyl ether and cooled at −5 °C to afford the product as white blocklike crystals (yield 52%). IR (Nujol mull): 1247 (vs) cm^{-1} ($\nu_{P=O}$). ^{1}H NMR ($CDCl_3$): δ 7.74 (m), 7.43 (m, 30 H, C_6H_5), 5.26 (s, 2 H, CH_2Cl_2). $^{31}P\{^1H\}$ NMR ($CDCl_3$): δ ($P(O)F_2$) 32.4 (tt, $^1J_{Pt-P}$ = 5761, $^1J_{P-F}$ = 1177, $^2J_{P-P}$ = 27.1 Hz), δ (PPh_3) 23.0 (dt, $^1J_{Pt-P}$ = 2555, $^2J_{P-P}$ = 27.1, $^3J_{P-F}$ = 10.0 Hz). The same species, identified by its characteristic ^{31}P NMR spectrum, is also present in the crude reaction mixture obtained in the synthesis of **2**. Anal. Calcd for $C_{37}H_{32}P_3F_2OCl_3Pt$: C, 48.04; H, 4.14; P, 10.04. Found: C, 48.0; H, 4.2; P, 9.5.

$Pt(\mu\text{-}CH_3N(PF_2)_2)_3Pt(P(C_6H_5)_3)$ (8). To an ethylene-saturated solution of 0.40 g (0.54 mmol) of $Pt(C_2H_4)(PPh_3)_2$ in 5 mL of toluene was added 0.1 mL (ca. 0.8 mmol) of $MeN(PF_2)_2$. The solution immediately turned orange and after several minutes had become yellow. After the solution was stirred at room temperature for 12 h the product had precipitated as pale yellow microcrystals. These were filtered off, washed with diethyl ether, and dried in vacuo (yield 0.3 g, 70%). The analytical sample was recrystallized from dichloromethane/hexane at −5 °C and obtained as bright yellow crystals. ^{1}H NMR ($CDCl_3$): δ 7.64 (m), 7.39 (m, 15 H, C_6H_5), 2.98 (t, J = 9.1 Hz, 9 H, NCH_3). $^{31}P\{^1H\}$ NMR ($CDCl_3$): δ (PPh_3) −13.6 (br, $^1J_{Pt-P}$ = 3056 Hz), δ (PNP) 116.9 (bt, $^1J_{Pt-P}$ 7330 Hz), 103.9 (bt, $^1J_{Pt-P}$ = 7615 Hz). Anal. Calcd for $C_{21}H_{24}P_7N_3F_{12}Pt_2$: C, 21.87; H, 2.10. Found: C, 21.8; H, 2.1.

$(\eta^5\text{-}C_5H_5)_2Mo_2(CO)_4(\mu\text{-}CH_3N(PF_2)_2)$ (9). To a solution of 0.229 g (0.446 mmol) of $cp_2Mo_2(CO)_4$ in 10 mL of toluene was added 0.08 g (0.50 mmol) of $MeN(PF_2)_2$. The brown solution immediately became dark red and was stirred at room temperature overnight. Following filtration through a pad of diatomaceous earth, the solution was concentrated under reduced pressure and diluted with hexane to afford the product as red microcrystals (yield 0.2 g, 77%). IR (CH_2Cl_2 solution): 1964 (m), 1927 (s), 1893 (m), 1880 (m), (ν_{CO}). ^{1}H NMR ($CDCl_3$): δ 5.17 (s, 10 H, C_5H_5), 2.90 (t, J = 8.2 Hz, 3 H, NCH_3). $^{31}P\{^1H\}$ NMR ($CDCl_3$): δ 195.8 ($X_2AA'X_2'$ pattern). Anal. Calcd for $C_{15}H_{13}P_2O_4NMo_2$: C, 29.97; H, 2.18; N, 2.33. Found: C, 29.9; H, 2.5; N, 2.2.

X-ray Crystallography. General procedures for crystal orientation, unit cell determination, and collection of intensity data on the CAD-4 diffractometer have been published.[12] All crystals were mounted on thin glass fibers and coated with epoxy cement to retard possible decomposition. All space groups were uniquely determined by the systematic absences observed in the final data sets. Intensity data were collected at ca. 296 K using graphite-monochromated, Mo Kα radiation (λ = 0.710 73 Å) in the $\omega/2\theta$ scan mode with a variable scan width of (0.80 + 0.20(tan θ))°. Raw intensities were corrected for Lorentz and polarization effects and absorption using ψ scans on several reflection with χ near 90°. For **4** an empirical absorption correction[18] was applied. All structures were solved by Patterson methods and developed by successive cycles of full-matrix, least-squares refinement and difference Fourier syntheses. The neutral atom-scattering factors used include the real and imaginary corrections for the effects of anomalous dispersion.[19] In the late stages of refinement, most hydrogen atoms could be seen in difference maps. These were included as fixed contributions in calculated positions (C–H = 0.95 Å) with isotropic temperature factors 1.2 times those of the attached carbon atoms and were updated periodically. In the final cycle, no parameter shifted by more than 10% of its standard deviation except for those associated with the disordered solvent in **2**. All final difference maps were essentially featureless except for **2** where a diffuse area of residual density remained which is presumably due to partial occupancy by highly disordered solvent molecules. All calculations were performed on a VAXstation 3100 with the MolEN[20] suite of programs. Crystallographic data specific to each determination are given in Table I, final atomic coordinates appear in Tables II–VI and the remaining data are included as supplementary material.

(18) Walker, N.; Stuart, D. *Acta Crystallogr.* **1983**, *A39*, 159.
(19) (a) Cromer, D. T.; Waber, J. T. *International Tables for X-ray Crystallography*; The Kynoch Press: Birmingham, England, 1974; Vol. IV, Table 2.2B. (b) Cromer, D. T. *International Tables for X-ray Crystallography*; The Kynoch Press: Birmingham, England, 1974, Vol. IV, Table 2.3.1.
(20) MolEN, An Interactive Structure Solution Procedure, Enraf-Nonius, Delft, The Netherlands, 1990.

Table II. Positional Parameters (Esd's) for $cpFe(MeN(PF_2)_2)_2Co(CO)_2$

atom	x	y	z	B (Å²)[a]
Co	0.23507 (7)	0.12578 (3)	0.40020 (6)	2.74 (1)
Fe	0.27920 (7)	0.13164 (3)	0.15082 (6)	2.69 (1)
P(1)	0.4694 (1)	0.11432 (6)	0.4469 (1)	2.89 (2)
P(2)	0.1667 (1)	0.22489 (6)	0.3641 (1)	3.24 (3)
P(3)	0.3684 (1)	0.22748 (6)	0.1879 (1)	2.60 (2)
P(4)	0.4830 (1)	0.08023 (7)	0.1972 (1)	3.33 (3)
F(1)	0.5230 (3)	0.0654 (1)	0.5580 (3)	4.54 (7)
F(2)	0.5725 (3)	0.1735 (2)	0.5041 (3)	5.07 (8)
F(3)	0.0003 (3)	0.2432 (2)	0.3066 (3)	5.78 (8)
F(4)	0.1624 (4)	0.2719 (2)	0.4806 (3)	5.61 (8)
F(5)	0.3753 (3)	0.2776 (1)	0.0770 (3)	3.98 (6)
F(6)	0.5390 (3)	0.2384 (1)	0.2437 (3)	4.00 (6)
F(7)	0.6203 (3)	0.0934 (2)	0.1177 (3)	5.77 (8)
F(8)	0.4820 (4)	0.0022 (2)	0.1745 (3)	5.71 (8)
O(1)	0.1467 (5)	0.1182 (2)	0.6527 (4)	7.0 (1)
O(2)	0.0958 (5)	−0.0013 (2)	0.3204 (4)	6.1 (1)
N(1)	0.5768 (4)	0.0864 (2)	0.3390 (4)	3.32 (9)
N(2)	0.2717 (4)	0.2741 (2)	0.2803 (4)	3.04 (8)
C(1)	0.1791 (6)	0.1221 (3)	0.5526 (5)	4.1 (1)
C(2)	0.1495 (6)	0.0499 (3)	0.3453 (5)	4.0 (1)
C(3)	0.0886 (6)	0.1663 (3)	0.0357 (5)	4.6 (1)
C(4)	0.2116 (7)	0.1546 (3)	−0.0349 (5)	5.1 (1)
C(5)	0.2475 (7)	0.0861 (3)	−0.0227 (6)	6.0 (1)
C(6)	0.1484 (7)	0.0558 (3)	0.0545 (6)	5.6 (1)
C(7)	0.0498 (6)	0.1056 (3)	0.0900 (6)	4.8 (1)
C(8)	0.7417 (6)	0.0692 (4)	0.3691 (7)	6.4 (2)
C(9)	0.2776 (6)	0.3480 (2)	0.2892 (5)	4.0 (1)

[a] Anisotropically refined atoms are given in the form of the isotropic equivalent displacement parameter defined as $B_{eq} = {}^4/_3[a^2B_{11} + b^2B_{22} + c^2B_{33} + ab(\cos\gamma)B_{12} + ac(\cos\beta)B_{13} + bc(\cos\alpha)B_{23}]$.

(a) $cpFe(MeN(PF_2)_2)_2Co(CO)_2$ (1). A dark red irregular plate (0.07 × 0.16 × 0.26 mm), obtained by slow crystallization of a concentrated hexane solution at −5 °C, was used. A correction for a 6.9% linear decay in the intensity monitors was applied to the intensity data.

(b) $cpFe(PF_2NHMe)(\mu\text{-}PF_2)(\mu\text{-}PF_2NMe)PtCl(PPh_3)$ (2). An amber block obtained by cooling a concentrated dichloromethane/hexane solution of the complex at −5 °C was cut to give a piece measuring 0.20 × 0.33 × 0.33 mm which was used for the data collection. Only statistical fluctuations were noted in the intensity standards. Equivalent data were averaged with an agreement factor of 0.017 on *F*. Although the hydrogen attached to nitrogen in the PF_2NHMe ligand was readily evident in a difference map, it could not be satisfactorily refined and so was placed in the location indicated by the difference map and allowed to ride on the nitrogen atom. In the late stages of the refinement, residual density in the difference map consisted of several small peaks, the largest of which was well-resolved, and a rather diffuse area of density nearby. This was assumed to be the residual dichloromethane of solvation indicated by the ^1H NMR of the crystal sample and from trial occupancy refinements the largest peak was judged to be a chlorine atom of ca. 40% occupancy. Careful inspection of a difference map obtained following inclusion of this atom suggested it to be part of a dichloromethane molecule in which the second chlorine atom is disordered over two alternate positions but these were poorly resolved and all attempts at their refinement were unsatisfactory. A reasonable compromise between locating the carbon atom and disordered chlorine atoms at the centers of the residual peaks and providing a reasonable geometry for the solvent molecule was made after several attempts, and the resulting atomic positions for the solvent were fixed for the remainder of the refinement. The remaining density, which could not be modeled satisfactorily, appears to be additional solvent at partial occupancy and disordered about the center of symmetry.

(c) $Pt(PPh_3)(\mu\text{-}MeN(PF_2)_2)_2Mo(CO)_3$ (4). Slow diffusion of hexane into a toluene solution of the crude material obtained from the reaction of $Mo(CO)_3MeN(PF_2)_2$ with $Pt(PPh_3)_2(C_2H_4)$ initially resulted in the formation of a dirty tan solid. After several weeks a few orange crystals formed on the side of the flask. An irregular fragment cut from one of these and measuring 0.2 × 0.33 × 0.33 mm was used for the data collection. The initial orthorhombic cell chosen by the CAD-4 software was shown by the systematic absences found in the final data set to be a nonstandard setting of the space group *Pbca*. Consequently the data were transformed to the standard setting and corrected for a linear 5.1% decrease in the intensity monitors.

Table III. Positional Parameters (Esd's) for $cpFe(PF_2NHMe)(\mu\text{-}PF_2)(\mu\text{-}PF_2NMe)PtCl(PPh_3)$

atom	x	y	z	B (Å²)[a]
Pt	0.23911 (2)	0.07088 (2)	0.27800 (1)	2.952 (5)
Fe	0.47611 (9)	0.23123 (9)	0.26874 (6)	3.90 (3)
Cl	0.0768 (2)	0.0264 (2)	0.2244 (1)	4.72 (5)
P(1)	0.3843 (2)	0.1343 (2)	0.3229 (1)	3.42 (4)
P(2)	0.3570 (2)	0.3387 (2)	0.2618 (1)	4.30 (5)
P(3)	0.4164 (2)	0.1530 (2)	0.1888 (1)	4.21 (5)
P(4)	0.1577 (2)	0.0314 (2)	0.3672 (1)	3.16 (4)
F(1)	0.3602 (4)	0.1839 (4)	0.3885 (2)	5.3 (1)
F(2)	0.4547 (4)	0.0478 (4)	0.3540 (3)	5.3 (1)
F(3)	0.3880 (5)	0.4353 (4)	0.2265 (4)	7.6 (2)
F(4)	0.3385 (5)	0.3985 (5)	0.3236 (3)	7.9 (2)
F(5)	0.4962 (5)	0.0738 (4)	0.1638 (3)	6.5 (1)
F(6)	0.4114 (5)	0.2135 (5)	0.1246 (3)	6.4 (1)
N(1)	0.2403 (6)	0.3184 (6)	0.2344 (4)	5.3 (2)
N(2)	0.3050 (6)	0.1011 (6)	0.1909 (3)	4.5 (2)
C(1)	0.1559 (9)	0.394 (1)	0.2282 (7)	8.2 (4)
C(2)	0.2600 (9)	0.0552 (9)	0.1319 (5)	6.8 (3)
C(3)	0.5968 (7)	0.2351 (9)	0.3372 (6)	6.8 (3)
C(4)	0.6257 (7)	0.1755 (8)	0.2904 (7)	7.2 (3)
C(5)	0.6267 (8)	0.239 (1)	0.2350 (7)	9.8 (4)
C(6)	0.5980 (9)	0.3338 (9)	0.2570 (7)	7.8 (3)
C(7)	0.5792 (8)	0.3289 (9)	0.3157 (7)	7.3 (3)
C(411)	0.2267 (6)	0.0434 (6)	0.4435 (4)	3.6 (2)
C(412)	0.3086 (7)	−0.0240 (8)	0.4573 (5)	4.6 (2)
C(413)	0.3660 (7)	−0.0183 (9)	0.5170 (5)	5.9 (2)
C(414)	0.3408 (9)	0.057 (1)	0.5596 (5)	7.0 (3)
C(415)	0.2609 (9)	0.121 (1)	0.5460 (5)	6.6 (3)
C(416)	0.2050 (7)	0.1140 (7)	0.4878 (5)	4.8 (2)
C(421)	0.1134 (6)	−0.0971 (6)	0.3702 (4)	3.5 (2)
C(422)	0.0724 (8)	−0.1329 (7)	0.4247 (5)	4.7 (2)
C(423)	0.0369 (9)	−0.2286 (7)	0.4273 (5)	6.2 (3)
C(424)	0.0472 (9)	−0.2919 (7)	0.3785 (5)	6.0 (3)
C(425)	0.0908 (8)	−0.2571 (7)	0.3246 (5)	5.8 (3)
C(426)	0.1241 (7)	−0.1623 (7)	0.3200 (4)	4.2 (2)
C(431)	0.0425 (6)	0.1116 (6)	0.3736 (4)	3.5 (2)
C(432)	0.0540 (7)	0.2085 (8)	0.3594 (5)	5.8 (2)
C(433)	−0.0283 (9)	0.2750 (8)	0.3633 (6)	6.5 (3)
C(434)	−0.1224 (8)	0.2433 (9)	0.3824 (6)	6.3 (3)
C(435)	−0.1343 (8)	0.1459 (9)	0.3985 (6)	6.6 (3)
C(436)	−0.0534 (7)	0.0795 (7)	0.3929 (5)	4.6 (2)
Cl(1S)	0.669	0.192	0.024	18.1*
Cl(2S)	0.480	0.147	−0.030	19.9*
Cl(3S)	0.714	0.033	0.025	19.9*
C(1S)	0.600	0.100	0.014	15.9*

[a] Starred atoms were refined isotropically. Anisotropically refined atoms are given in the form of the isotropic equivalent displacement parameter defined as $B_{eq} = {}^4/_3[a^2B_{11} + b^2B_{22} + c^2B_{33} + ab(\cos\gamma)B_{12} + ac(\cos\beta)B_{13} + bc(\cos\alpha)B_{23}]$.

(d) $PtCl(P(O)F_2)(PPh_3)_2\cdot CH_2Cl_2$ (7). Colorless crystals obtained by slow diffusion of hexane into a dichloromethane solution of the complex had the appearance of pointed columns and were twinned parallel to the column axis. A well-formed crystal in which the twinning plane was sharply defined under the polarizing microscope was cleaved to give a single crystal measuring 0.33 × 0.16 × 0.53 mm. Only statistical fluctuations in the intensity monitors was observed during the data collection. As the Patterson map indicated that the platinum atom lies on a center of symmetry, the Cl and $P(O)F_2$ ligands are statistically disordered. The chlorine and phosphorus (P_2) atoms were therefore assigned essentially equivalent positions with occupancies of 0.5 and refined alternately. The half-occupancy fluorine and oxygen atoms were readily located and refined satisfactorily. Also located was an ordered molecule of dichloromethane which was given an occupancy of 0.5 on the basis of trial refinements of the occupancy factor.

(e) $Pt_2(MeN(PF_2)_2)_3(PPh_3)$ (8). A bright-yellow, multifaceted

Table IV. Positional Parameters (Esd's) for $(Ph_3P)Pt(\mu\text{-}MeN(PF_2)_2)_2Mo(CO)_3$

atom	x	y	z	B (Å²)[a]
Pt	0.16118 (4)	0.10324 (2)	0.07825 (3)	3.37 (1)
Mo	0.2028 (1)	−0.00786 (6)	0.14298 (7)	4.11 (3)
P(1)	0.1680 (3)	0.2027 (2)	0.0610 (2)	3.04 (8)
P(2)	0.2995 (3)	0.0823 (2)	0.0374 (2)	4.03 (9)
P(3)	0.0185 (3)	0.0890 (2)	0.1129 (2)	4.08 (9)
P(4)	0.0468 (3)	−0.0297 (2)	0.1323 (3)	5.1 (1)
P(5)	0.3577 (3)	0.0176 (2)	0.1463 (3)	5.8 (1)
F(1)	0.3465 (6)	0.1337 (4)	−0.0013 (5)	5.8 (2)
F(2)	0.3002 (6)	0.0405 (4)	−0.0285 (5)	5.5 (2)
F(3)	−0.0121 (7)	0.1224 (4)	0.1788 (5)	7.4 (3)
F(4)	−0.0549 (6)	0.1146 (4)	0.0636 (6)	6.7 (3)
F(5)	−0.0021 (8)	−0.0638 (5)	0.1919 (6)	9.0 (3)
F(6)	0.0102 (8)	−0.0705 (5)	0.0739 (7)	9.3 (3)
F(7)	0.4048 (9)	0.0472 (6)	0.2088 (6)	10.2 (4)
F(8)	0.4339 (8)	−0.0301 (5)	0.1370 (7)	10.6 (4)
O(3)	0.252 (1)	−0.0875 (5)	0.0161 (7)	8.6 (4)
O(4)	0.235 (1)	−0.1155 (6)	0.2356 (8)	9.8 (4)
O(5)	0.166 (1)	0.0633 (7)	0.2781 (7)	9.8 (5)
N(1)	0.3887 (9)	0.0635 (5)	0.0824 (7)	4.8 (3)
N(2)	−0.0267 (9)	0.0242 (5)	0.1261 (6)	4.5 (3)
C(1)	0.486 91)	0.081 (1)	0.069 (1)	9.0 (7)
C(2)	−0.129 (1)	0.0158 (9)	0.127 (1)	7.1 (5)
C(3)	0.231 (1)	−0.0584 (6)	0.0599 (8)	4.7 (4)
C(4)	0.222 (1)	−0.0771 (7)	0.2026 (9)	6.4 (4)
C(5)	0.177 (1)	0.0389 (7)	0.2285 (8)	5.7 (5)
C(11)	0.0836 (9)	0.2507 (7)	0.1003 (7)	3.1 (3)
C(12)	−0.006 (1)	0.2463 (6)	0.0802 (9)	4.5 (3)
C(13)	−0.071 (1)	0.2818 (7)	0.1061 (9)	5.4 (4)
C(14)	−0.049 (1)	0.3226 (7)	0.156 (1)	5.9 (4)
C(15)	0.039 (1)	0.3303 (7)	0.1756 (9)	5.6 (4)
C(16)	0.107 (1)	0.2907 (8)	0.1502 (9)	5.1 (4)
C(21)	0.1688 (9)	0.2274 (6)	−0.0282 (7)	3.1 (3)
C(22)	0.173 (1)	0.1876 (7)	−0.0815 (9)	4.7 (4)
C(23)	0.176 (1)	0.2076 (8)	−0.1497 (8)	5.5 (4)
C(24)	0.176 (1)	0.2648 (9)	−0.1633 (9)	7.0 (5)
C(25)	0.174 (1)	0.3054 (7)	−0.1104 (9)	5.6 (4)
C(26)	0.167 (1)	0.2866 (7)	−0.0437 (8)	4.8 (4)
C(31)	0.2759 (9)	0.2263 (6)	0.0988 (8)	3.7 (3)
C(32)	0.298 (1)	0.2006 (7)	0.1618 (9)	5.4 (4)
C(33)	0.377 (1)	0.215 (1)	0.197 (1)	7.6 (6)
C(34)	0.430 (1)	0.259 (1)	0.170 (1)	8.2 (6)
C(35)	0.412 (1)	0.2852 (9)	0.107 (1)	6.9 (5)
C(36)	0.334 (1)	0.2695 (7)	0.0728 (9)	5.2 (4)

[a] Anisotropically refined atoms are given in the form of the isotropic equivalent displacement parameter defined as $B_{eq} = {}^4/_3[a^2B_{11} + b^2B_{22} + c^2B_{33} + ab(\cos\gamma)B_{12} + ac(\cos\beta)B_{13} + bc(\cos\alpha)B_{23}]$.

crystal, 0.23 × 0.26 × 0.40 mm, obtained by cooling a dichloromethane/hexane solution of the complex was used. The intensity data were corrected for a 2% linear decay in the intensity standards, and equivalent reflections were averaged resulting in an agreement factor of 0.015 on F.

Results and Discussion

Chemistry of $cpFeCl(PNP)_2$. From the work on this complex it appears that the predominant mode of reaction of $cpFeCl(PNP)_2$ with low-valent metal complexes involves, in effect, the transfer of chloride from iron to the low-valent metal, possibly in an initial PNP-bridged species, as has been observed previously for reactions with Rh(I) and Ir(I) complexes.[8] Thus the reaction of $cpFeCl(PNP)_2$ with an equimolar quantity of $Co_2(CO)_8$ in toluene/hexane results in the immediate evolution of CO and the formation of a blue solid identified as $CoCl_2$. Workup of the purple supernatant afforded dark, red-purple crystals characterized by elemental analysis, spectroscopic properties, and a single-crystal structure determination as $cpFe(\mu\text{-}PNP)_2Co(CO)_2$ (1). On the basis of these observations we tentatively suggest that the overall

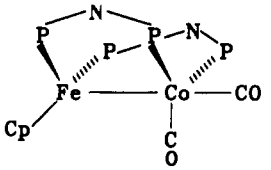

1

reaction is

$$2cpFeCl(PNP)_2 + {}^3/_2Co_2(CO)_8 \rightarrow CoCl_2 + 2cpFe(\mu\text{-}PNP)_2Co(CO)_2 + 8CO$$

The ^{31}P NMR spectrum of 1 consists of two triplets of multiplets with the upfield resonance being quite broad and poorly resolved. As quadrupole broadening is generally observed in the resonances of phosphorus bound to cobalt, this resonance is assigned to the phosphorus atoms on cobalt. The major triplet pattern is characteristic of all PNP complexes and arises primarily from $^1J_{P-F}$,[21] but because of the large number of spins involved it was not possible with the NMR spectral simulation programs available to us to perform a full analysis of the ^{31}P NMR spectrum.

In the reaction of $cpFeCl(PNP)_2$ with $Pt(C_2Ph_2)(PPh_3)_2$ not only does chloride transfer from iron to platinum occur but also the PNP ligands undergo fragmentation. This has been noted previously in some reactions involving PNP[6c,21-23] but is somewhat surprising in the present case since considerable care was taken to exclude moisture and the reaction medium is nonpolar. An in situ $^{31}P\{^1H\}$ NMR spectrum of the crude reaction mixture following removal of the bulk of the solvent in vacuo suggests that at least three significant products are formed. One of these, obtained in low yield following extensive chromatographic separation, has been identified by a single-crystal structure determination as $PtCl(PPh_3)(\mu\text{-}PF_2)(\mu\text{-}N(Me)PF_2)Fe(PF_2NHMe)cp$ (2) while a second, identified here by its

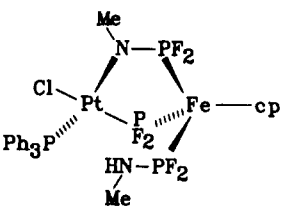

2

^{31}P NMR spectrum and prepared and fully characterized independently (vide infra), is *trans*-$PtCl(P(O)F_2)(PPh_3)_2$ (7). The remaining species produced have not been identified. The most striking feature of the ^{31}P NMR spectrum of 2 is a very-low-field (δ 290.0) resonance appearing as a triplet of doublets of doublets with well-resolved ^{195}Pt satellites which is assigned to the μ-PF_2 group. This chemical shift lies at about the middle of the large range previously determined for the μ-PF_2 ligand in homo- and heterobimetallic complexes (e.g. δ 177.2 in *cis*-$PtCl_2((\mu\text{-}PF_2)IrCl_2(CO)(PEt_3)_2)_2$[24] and δ 461.4 in $cpCr(CO)_3(\mu\text{-}PF_2)Cr(CO)_5$[25] and is closest to that found in $IrCl_2(CO)$

(21) King, R. B.; Lee, T. W. *Inorg. Chem.* **1982**, *21*, 319.
(22) Newton, M. G.; King, R. B.; Chang, M.; Gimeno, J. *J. Am. Chem. Soc.* **1978**, *100*, 326.
(23) Newton, M. G.; King, R. B.; Chang, M.; Gimeno, J. *J. Am. Chem. Soc.* **1978**, *100*, 1632.
(24) Ebsworth, E. A. V.; Gould, R. O.; McManus, N. T.; Rankin, D. W. H.; Walkinshaw, M. D.; Whitelock, J. D. *J. Organomet. Chem.* **1983**, *249*, 227.

Table V. Positional Parameters (Esd's) for $PtCl(P(O)F_2)(PPh_3)_2$

atom	x	y	z	B (Å²)[a]
Pt	0.000	0.500	0.500	3.416 (8)
Cl	0.098	0.407	0.475	7.2
P(1)	0.1372 (2)	0.5626 (1)	0.3871 (3)	3.41 (4)
P(2)	−0.1175 (4)	0.5865 (2)	0.4986 (6)	5.0 (1)
F(1)	−0.229 (1)	0.5796 (7)	0.383 (2)	8.4 (4)
F(2)	−0.153 (1)	0.5966 (5)	0.667 (1)	6.5 (3)
O	−0.062 (1)	0.6493 (5)	0.463 (1)	4.2 (2)
C(11)	0.0739 (7)	0.6157 (4)	0.234 (1)	3.8 (2)
C(12)	−0.0116 (8)	0.5918 (5)	0.125 (1)	4.9 (2)
C(13)	−0.063 (1)	0.6301 (5)	0.006 (1)	5.8 (3)
C(14)	−0.031 (1)	0.6949 (6)	−0.006 (1)	6.3 (3)
C(15)	0.050 (1)	0.7185 (5)	0.100 (1)	6.0 (3)
C(16)	0.1032 (8)	0.6806 (5)	0.225 (1)	4.9 (2)
C(21)	0.2471 (8)	0.5222 (6)	0.286 (1)	4.7 (2)
C(22)	0.242 (1)	0.5177 (6)	0.119 (1)	5.3 (2)
C(23)	0.327 (1)	0.4829 (7)	0.050 (2)	7.7 (3)
C(24)	0.416 (1)	0.4545 (7)	0.149 (2)	9.5 (4)
C(25)	0.415 (1)	0.4593 (9)	0.305 (2)	10.5 (4)
C(26)	0.334 (1)	0.4895 (6)	0.380 (2)	7.8 (3)
C(31)	0.2168 (7)	0.6112 (4)	0.538 (1)	4.0 (2)
C(32)	0.3159 (9)	0.6442 (6)	0.501 (1)	5.8 (3)
C(33)	0.3769 (9)	0.6823 (6)	0.614 (1)	6.7 (3)
C(34)	0.3464 (9)	0.6849 (5)	0.767 (1)	6.2 (3)
C(35)	0.249 (1)	0.6505 (6)	0.809 (1)	6.3 (3)
C(36)	0.1874 (8)	0.6139 (5)	0.696 (1)	4.8 (2)
C(1S)	0.314 (3)	0.189 (1)	0.277 (4)	9.1 (8)*
Cl(1S)	0.4552 (5)	0.1589 (4)	0.2844 (9)	9.3 (2)
Cl(2S)	0.3135 (5)	0.2710 (4)	0.272 (1)	9.4 (2)

[a] Starred atoms were refined isotropically. Anisotropically refined atoms are given in the form of the isotropic equivalent displacement parameter defined as $B_{eq} = {}^4/_3[a^2B_{11} + b^2B_{22} + c^2B_{33} + ab(\cos\gamma)B_{12} + ac(\cos\beta)B_{13} + bc(\cos\alpha)B_{23}]$.

$(PEt_3)_2(\mu\text{-}PF_2)RuCl_2(p\text{-cymene})$ (δ 252.6).[24] The triplet splitting is again due to $^1J_{P-F}$, and the approximate value of 1142 Hz is only slightly larger than the value of 1111 Hz seen in *cis*-$PtCl_2[(\mu\text{-}PF_2)IrCl_2(CO)(PEt_3)_2]_2$.[24] The additional splittings are most likely due to two-bond couplings to two of the remaining three phosphorus atoms, and we tentatively suggest that these are the ones bound to iron since $^2J_{P-P}$(cis) in square-planar Pt(II) complexes can be very small.[26] Unfortunately we were not able to reliably identify these couplings in the resonances assigned to the phosphorus atoms on iron because all resonances are distinctly second-order patterns and the number of spins present is beyond the capacity of the available spectral simulation program. The value of $^1J_{Pt-P}$ (3732 Hz) is slightly larger than typical values (3500–3600 Hz) for a variety of *cis*-$PtCl_2L_2$ (L = phosphine) complexes,[26,27] considerably larger than that in *cis*-$PtCl_2((\mu\text{-}PF_2)IrCl_2(CO)(PEt_3)_2)_2$ (3360 Hz)[24] and much less than those in $PtCl_2(PEt_3)(\mu\text{-}PF_2)PtCl(PEt_3)_2$ (4452, 4519 Hz).[28] While the Pt–PF_2 distances and Pt–PF_2–M angles in **2** and *cis*-$PtCl_2((\mu\text{-}PF_2)IrCl_2(CO)(PEt_3)_2)_2$ are comparable, there is sufficient difference in the identity of the second metal and the ligands on it and on Pt in these three complexes that it is difficult to draw any firm conclusions as to the factor(s) responsible for the observed differences in $^1J_{Pt-P}$. Nonetheless the value observed for **2** is clearly consistent with the platinum being Pt(II). The proton resonances at δ 3.65 and 2.35 are respectively assigned to the methyl

Table VI. Positional Parameters (Esd's) for $Pt_2(MeN(PF_2)_2)_3(PPh_3)$

atom	x	y	z	B (Å²)[a]
Pt(1)	−0.02257 (2)	0.03070 (2)	0.25981 (1)	3.343 (6)
Pt(2)	0.21055 (2)	0.06482 (1)	0.23900 (1)	2.142 (4)
P(1)	−0.1155 (2)	0.0469 (1)	0.1394 (1)	3.26 (4)
P(2)	0.0134 (2)	−0.0931 (1)	0.3030 (1)	4.24 (4)
P(3)	−0.0233 (2)	0.1218 (2)	0.3490 (1)	4.44 (4)
P(4)	0.1018 (1)	0.1157 (1)	0.12833 (9)	2.45 (3)
P(5)	0.2218 (2)	−0.0710 (1)	0.2507 (1)	3.16 (4)
P(6)	0.2178 (2)	0.1323 (1)	0.34932 (9)	3.39 (4)
P(7)	0.4004 (1)	0.0942 (1)	0.22453 (9)	2.44 (3)
F(11)	−0.2272 (3)	0.1027 (3)	0.1157 (3)	5.2 (1)
F(12)	−0.1743 (4)	−0.0244 (3)	0.0862 (3)	5.5 (1)
F(21)	0.0147 (5)	−0.1195 (3)	0.3874 (3)	6.9 (1)
F(22)	−0.0662 (4)	−0.1657 (3)	0.2628 (3)	6.7 (1)
F(31)	−0.0528 (4)	0.0949 (4)	0.4265 (3)	7.5 (1)
F(32)	−0.1052 (4)	0.1979 (4)	0.3389 (3)	6.9 (1)
F(41)	0.0842 (4)	0.2097 (2)	0.1214 (2)	4.5 (1)
F(42)	0.1598 (3)	0.1102 (3)	0.0572 (2)	4.16 (9)
F(51)	0.3468 (4)	−0.1055 (3)	0.2880 (3)	6.3 (1)
F(52)	0.2057 (5)	−0.1217 (3)	0.1733 (3)	6.2 (1)
F(61)	0.2932 (4)	0.2101 (3)	0.3608 (3)	7.4 (1)
F(62)	0.2888 (4)	0.0901 (4)	0.4241 (2)	7.3 (1)
N(1)	−0.0332 (5)	0.0862 (4)	0.0835 (3)	3.5 (1)
N(2)	0.1448 (5)	−0.1280 (4)	0.2992 (3)	3.8 (1)
N(3)	0.1063 (5)	0.1677 (4)	0.3817 (3)	4.7 (1)
C(1)	−0.0826 (7)	0.1074 (6)	0.0024 (4)	5.2 (2)
C(2)	0.1835 (8)	−0.2113 (5)	0.3254 (5)	5.1 (2)
C(3)	0.1248 (9)	0.2281 (7)	0.4460 (5)	8.9 (3)
C(4)	0.4122 (5)	0.1837 (4)	0.1668 (3)	2.9 (1)
C(5)	0.3535 (7)	0.2544 (5)	0.1768 (4)	4.0 (2)
C(6)	0.3644 (7)	0.3228 (5)	0.1354 (5)	5.0 (2)
C(7)	0.4333 (8)	0.3214 (5)	0.0817 (4)	4.9 (2)
C(8)	0.4916 (7)	0.2532 (5)	0.0723 (4)	5.0 (2)
C(9)	0.4840 (6)	0.1837 (5)	0.1142 (4)	4.3 (2)
C(10)	0.5085 (5)	0.1128 (4)	0.3144 (3)	2.9 (1)
C(11)	0.5761 (6)	0.1830 (5)	0.3288 (4)	4.2 (2)
C(12)	0.6572 (6)	0.1947 (6)	0.3961 (4)	4.9 (2)
C(13)	0.6761 (7)	0.1340 (6)	0.4510 (5)	5.9 (2)
C(14)	0.6095 (7)	0.0669 (6)	0.4401 (4)	5.0 (2)
C(15)	0.5261 (6)	0.0549 (5)	0.3726 (4)	4.3 (2)
C(16)	0.4669 (5)	0.0141 (4)	0.1779 (3)	2.7 (1)
C(17)	0.4013 (6)	−0.0161 (5)	0.1077 (4)	3.9 (2)
C(18)	0.4474 (7)	−0.0771 (5)	0.0697 (4)	4.9 (2)
C(19)	0.5572 (6)	−0.1080 (5)	0.1004 (4)	4.6 (2)
C(20)	0.6215 (6)	−0.0783 (5)	0.1696 (4)	4.4 (2)
C(21)	0.5798 (6)	−0.0158 (5)	0.2087 (4)	3.7 (2)

[a] Anisotropically refined atoms are given in the form of the isotropic equivalent displacement parameter defined as $B_{eq} = {}^4/_3[a^2B_{11} + b^2B_{22} + c^2B_{33} + ab(\cos\gamma)B_{12} + ac(\cos\beta)B_{13} + bc(\cos\alpha)B_{23}]$.

groups of the PF_2NMe and PF_2NHMe ligands on the basis of the coupling patterns. The doublet of doublets splitting for the latter is consistent with coupling of the methyl protons to the N–H proton and to phosphorus. Similar spectra have been previously reported for $Fe(CO)_4(PF_2NHMe)$[29] and $Mo_2(\mu\text{-}Cl)(\mu\text{-}PF_2)(\mu\text{-}PNP)_2(CO)_3(PF_2NHMe)$.[6c] The N–H stretching vibration is observed at 3295 cm^{-1} which is considerably lower than the values of 3440 and 3430 cm^{-1} observed respectively for the iron and molybdenum complexes just mentioned. We suggest that this may reflect a weak interaction of the N–H moiety with platinum as suggested by the structure study (vide infra).

Despite the apparent complexity of the reaction leading to **2**, some suggestions about its course are possible. That both **2** and **7** are observed in the original reaction mixtures *before* chromatographic workup clearly indicates that fragmentation of the PNP ligand occurs in the course of the reaction and not on the column. Also, since no indi-

(25) Malish, W.; Panster *Agnew. Chem. Int. Ed. Engl.* **1977**, *16*, 408.
(26) Pregosin, P. S.; Kunz, R. W. *NMR Basic Principles and Progress*; Diehl, P., Fluck, E., Kosfield, R., Eds.; Springer-Verlag: New York, 1979; Vol. 16 (^{31}P and ^{13}C NMR of Transition Metal Complexes).
(27) Verkade, J. G.; Mosbo, J. *Phosphorus-31 NMR Spectroscopy in Stereochemical Analysis*; Verkade, J. G., Quin, L. D., Eds.; VCH Publishers, Inc.: Deerfield Beach, FL, 1987; Chapter 13.
(28) Ebsworth, E. A. V.; Rankin, D. W. H.; Whitlock, J. D. *J. Chem. Soc., Dalton Trans.* **1981**, 840.
(29) King, R. B.; Lee, T. W.; Kim, J. H. *Inorg. Chem.* **1983**, *22*, 2964.

cation of PNP cleavage and/or oxidation of platinum occurs in the reaction of PNP itself with $Pt(L)(PPh_3)_2$ (L = C_2H_4, C_2Ph_2) (vide infra) under comparable conditions, it is reasonable to suggest that the cleavage occurs after the platinum is at least partially oxidized. Thus transfer of chloride from iron to platinum would give a formally Pt(I) species which could then be involved in an oxidative cleavage of one PNP ligand to generate the $\{PF_2\}$ and $\{PF_2NMe\}$ moieties as has been suggested to occur in the formation of $cp_2Fe_2(PNP)_2(\mu\text{-}PF_2)(\mu\text{-}PF_2NMe)$.[23]

Reactions of $cpFeCl(PNP)_2$ with several other complexes were explored but in no instances was a characterizable, heterobimetallic complex obtained. With $CoH(N_2)(PPh_3)_3$ only intractable solids resulted while with $PtCl_2(NCPh)_2$ the major product was a highly insoluble, dark bluish green solid. Given the tendency of $cpFeCl(PNP)_2$ to function, in effect, as an oxidizing agent it is likely that the solid is a partially oxidized, polymeric platinum species of the type generally referred to as platinum "blue". Onyl partial reaction occurred with $Ni(CO)_2(PPh_3)_2$ at room temperature and at 60 °C as resonances attributable to both starting complexes were seen in the ^{31}P NMR spectrum of the crude reaction mixtures. Also evident were resonances due to free triphenylphosphine, the previously reported $Ni_2(CO)_2(\mu\text{-}CO)(\mu\text{-}PNP)_2$,[7] and a singlet at δ 40.0 which we tentatively ascribe to $Ni(CO)_3(PPh_3)$.[30]

Chemistry of *fac*-$Mo(CO)_3(PNP)_2$. Reaction of *fac*-$Mo(CO)_3(PNP)_2$ with $Ni(CO)_2(PPh_3)_2$ and with $Pt(C_2H_4)(PPh_3)_2$ forms yellow products formulated as $Mo(CO)_3(\mu\text{-}PNP)M(PPh_3)$ (M = Ni (**3**), Pt (**4**)). The structure of **4** has been determined by X-ray crystallography (Figure 3) and although we have been unable to obtain satisfactory elemental analysis, presumably due to the repeated presence of excess triphenylphosphine in even the recrystallized samples, the spectroscopic properties of the bulk sample (vide infra) are consistent with the X-ray structure. Complex **3** analyzes satisfactorily for the formulation given above and its spectroscopic data indicate that it has a comparable structure. Thus **3** exhibits three carbonyl absorptions consistent with the presence of a *mer*-$\{Mo(CO)_3\}$ moiety which are of sufficiently high energy that no semibridging interactions are present. The triphenylphosphine ligand shows the expected triplet resonance, but unlike most of the other heterobimetallic complexes reported here, separate triplet of multiplet resonances for the PNP phosphorus atoms are not seen. Rather this portion of the ^{31}P NMR spectrum consists of a pattern of ten peaks, each showing additional fine structure, which, neglecting the fine structure, is symmetrical about the pattern center. It appears very much like a typical AA'BB' pattern and suggests that the chemical shifts of the molybdenum- and nickel-bound phosphorus atoms are not very much different. The greater complexity of the upfield half of the pattern suggests additional couplings (to triphenylphosphine) consistent with assignment of the higher chemical shift to the PNP phosphorus atoms bound to nickel.

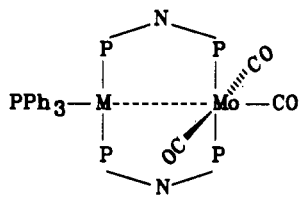

3. M = Ni
4. M = Pt

The $^{31}P\{^1H\}$ NMR spectrum of **4** at 298 K consists of a broad singlet at δ 27.7 and a complex pattern centered at δ 172 having the appearance of two nearly coincident triplets of multiplets and possessing ^{195}Pt satellites. On cooling, the upfield resonance broadens and at 202 K becomes resolved into rather broad singlets at δ 31.4 and −4.0 with the former having ca. six times the intensity of the latter and now also showing well-resolved ^{195}Pt satellites. Concomitantly the downfield multiplet shows a broadening and then a resharpening of some of the component lines as the temperature is lowered, but the ^{195}Pt satellites remain. The δ −4.0 resonance indicates the presence of a small quantity of free triphenylphosphine (confirmed by measurement of an authentic sample) while that at δ 31.4 is assigned to triphenylphosphine coordinated to platinum. The low-temperature spectrum is fully consistent with the X-ray structure, and while the lack of observable coupling between the PNP and triphenylphosphine ligands is somewhat surprising, we note that a similar situation is seen in **8**. The breadth of the upfield phosphorus resonance in the room temperature spectrum and its lack of ^{195}Pt satellites can be attributed to intermolecular exchange of triphenylphosphine on platinum.

With $IrCl(CO)(PPh_3)_2$, the molybdenum complex yields orange-yellow crystals analyzing as $IrMoCl(CO)_4(PNP)_2(PPh_3)$ (**5**). The infrared spectrum in the carbonyl region is very similar to that of **4** but with a fourth band at 1989 cm^{-1}, indicating the presence of *mer*-$\{Mo(CO)_3\}$ moiety and retention of the terminal carbonyl group on iridium. The ^{31}P NMR spectrum shows two well-separated triplet of multiplets resonances at low field and an upfield triplet which can be assigned respectively to the PNP and triphenylphosphine ligands. These data suggest that **5** has the structure

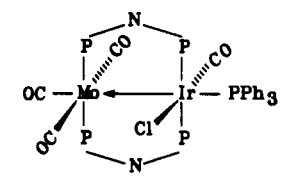

5

Without a value for the Ir–Mo separation the extent of metal–metal interaction cannot be determined, but by analogy with the argument made for **4** (vide infra) at least a weak Ir → Mo donor interaction is plausible.

With $RhCl(CO)(PPh_3)_2$ the molybdenum complex yields bright orange crystals analyzing as $RhMoCl(CO)_3(PNP)_2(PPh_3)\cdot 2CH_2Cl_2$ (**6**). The presence of the solvent dichloromethane was confirmed by the ^1H NMR spectrum. Unexpectedly the infrared spectrum in the carbonyl region is not comparable to those of **4** or **5**—in particular the strong band above 2000 cm^{-1} is absent—but rather resembles that of the parent molybdenum complex with the three-band pattern shifted to lower energy, suggesting retention of *fac* stereochemistry for the $\{Mo(CO)_3\}$ moiety. Repeated attempts to determine the structure of **6** have been frustrated by poor crystal quality, crystal decomposition, and extensive disorder. The best results to date show **6** to crystallize in the cubic space group *Pa*3 with the molecule lying on the crystallographic 3-fold axis. The metal atoms, the phosphorus atom of the triphenylphosphine ligand and the axial carbonyl group on molybdenum lie on the axis and are ordered but the remaining ligands suffer a 3-fold disorder which has prevented a full solution. Reasonable locations for the PNP phosphorus

(30) Meriwether, L. S.; Leto, J. R. *J. Am. Chem. Soc.* **1961**, *83*, 3192.

atoms and the chloride ligand could be defined, but the disordered locations of the remaining atoms of the PNP ligands and the equatorial carbonyl groups overlap to such an extent that further resolution of the disorder proved impossible. On the basis of the partial solution we tentatively propose that **6** has the structure

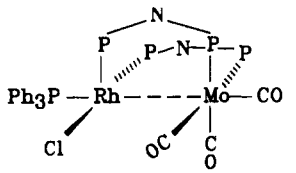

6

With a Rh–Mo separation of ca. 3.0 Å, metal–metal interaction is, at best, weak. Consistent with the proposed structure, the ^{31}P NMR spectrum is significantly different from those of **5** and $RhMo(CO)_2(\mu\text{-}Cl)(\mu\text{-}CO)(\mu\text{-}MeN(P(OPr^i)_2)_2)_2$.[3b] Instead of two well-separated triplet of multiplets resonances for the PNP ligands the spectrum consists of what appears to be a more complex triplet of multiplets pattern partially overlapped on the upfield side by two more closely spaced triplets of multiplets. We assign the first to the Mo-bound phosphorus atoms and the other two to those on rhodium which would be expected to be nonequivalent in the proposed structure. Well upfield is a broad (ca. 125 Hz) resonance attributable to the triphenylphosphine ligand in which some poorly resolved coupling is evident. The whole spectrum is invariant over the range 298–208 K, so the breadth of the upfield peak is probably due to unresolved Rh–P, P–P, and P–F couplings rather than to dynamic processes.

Reaction of $Mo(CO)_3(PNP)_2$ with $(RhCl(CO)_2)_2$ does not yield a heterobimetallic complex. Instead transfer of PNP ligands from molybdenum to rhodium occurs and the major product isolated is the known complex $(Rh(\mu\text{-}Cl)(\mu\text{-}PNP))_3$[6a,b] which was identified by its ^{31}P NMR spectrum.

Miscellaneous Reactions. The complex characterized as $PtCl(P(O)F_2)(PPh_3)_2$ (**7**) and identified as a coproduct with **2** (vide supra) can be prepared directly and in good yield from PNP and $PtCl_2(PPh_3)_2$ in dichloromethane. It has been previously reported as the product of a Michaelis–Arbusov reaction between $PtCl_2(PPh_3)_2$ and alkoxydifluorophosphines.[31] In the present case the source of oxygen for generation of the difluorophosphonate ligand is probably adventitious moisture. Whether this by itself can be responsible for the initial cleavage of the PNP is uncertain but if the reaction proceeds via initial replacement of chloride by PNP on platinum by analogy with the mechanism proposed for the alkoxydifluorophosphine reaction[31] then the presence of chloride ion and traces of moisture may generate sufficient acid to cleave the P–N bond as has been noted in some molybdenum systems.[6c] The spectroscopic data obtained for **7** compare well with the limited data reported previously[31] and in addition we have obtained the complete ^{31}P NMR spectrum (see Experimental Section). All the chemical shifts and coupling constants compare well with those for related complexes.

As an aid to the interpretation of the ^{31}P NMR spectra obtained, particularly for the platinum systems, in the reactions described above, several other reactions of PNP itself were undertaken. High yields of a bright yellow, air-stable complex characterized by elemental analysis and a single-crystal structure determination as $Pt_2(\mu\text{-}PNP)_3$-

(31) Grosse, J.; Schmutzler, R. *J. Chem. Soc., Dalton Trans.* **1976**, 405.

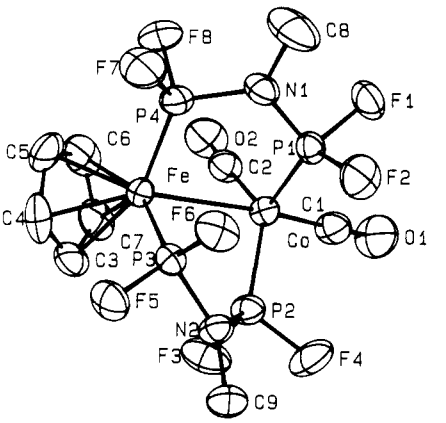

Figure 1. A perspective view of $cpFe(\mu\text{-}PNP)_2Co(CO)_2$ (**1**). Thermal ellipsoids are drawn at the 50% probability level. Hydrogen atoms are omitted for clarity.

(PPh_3) (**8**) are obtained from PNP and $Pt(C_2H_4)(PPh_3)_2$ in toluene. The ^{31}P NMR spectrum consists of two broad,

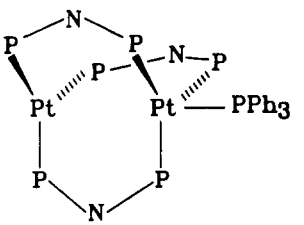

8

overlapping triplet patterns for the PNP ligands and a narrower multiplet for PPh_3 all having ^{195}Pt satellites. The value of $^1J_{Pt\text{-}P}$ for the triphenylphosphine ligand (3056 Hz) is close to that reported for the tripod phosphorus ligand in $Pt((Ph_2PCH_2)_3CCH_3)(PF_2N(CH_3)_2)$ (2893 Hz) while those for the PNP ligands (7330, 7615 Hz), although significantly smaller than the value of 8838 Hz for the $PF_2N(CH_3)_2$ ligand in the same complex are nonetheless quite large as expected.[32]

Reaction of PNP with $cp_2Mo_2(CO)_4$ readily affords a red product characterized by elemental analysis and spectroscopic data as $cp_2Mo_2(CO)_4(\mu\text{-}PNP)$ (**9**). In particular, the ^{31}P NMR spectrum of **9** is a symmetrical pattern of the $X_2AA'X'_2$ type seen for the free ligand itself and in a variety of other PNP complexes where PNP is symmetrically coordinated, indicating that both phosphorus atoms are chemically equivalent. Also the observation of a single cyclopentadienyl resonance indicates that the PNP is bound to both metals.

Description of Structures. (a) $cpFe(\mu\text{-}MeN(PF_2)_2)_2Co(CO)_2$ (1). A perspective view of **1** is shown in Figure 1 and pertinent bond distances and interbond angles appear in Table VII. There are no unusual intermolecular contacts in the solid. The Co–Fe distance of 2.743 (1) Å is considerably longer than those found previously in a variety of binuclear and cluster Fe/Co complexes (2.45–2.67 Å)[33-44] but is only modestly longer than

(32) Chatt, J.; Mason, R.; Meek, D. W. *J. Am. Chem. Soc.* **1975**, *97*, 3926.
(33) Keller, E.; Vahrenkamp, H. *Chem. Ber.* **1977**, *110*, 430.
(34) Keller, E.; Vahrenkamp, H. *Chem. Ber.* **1979**, *112*, 2347.
(35) Röttinger, E.; Trenkle, A.; Müller, R.; Vahrenkamp, H. *Chem. Ber.* **1980**, *113*, 1280.
(36) Keller, E.; Vahrenkamp, H. *Chem. Ber.* **1980**, *114*, 1111.
(37) Stephens, F. S. *J. Chem. Soc., Dalton Trans.* **1974**, 13.
(38) Davies, G.; Stephens, F. S. *J. Chem. Soc., Dalton Trans.* **1974**, 698.
(39) Campbell, I. L. C.; Stephens, F. S. *J. Chem. Soc., Dalton Trans.* **1974**, 923.

Table VII. Selected Bond Distances (Å) and Interbond Angles (deg) for cpFe(MeN(PF$_2$)$_2$)$_2$Co(CO)$_2$ (1)

Bond Distances			
Co–Fe	2.743 (1)	Fe–C(3)	2.086 (5)
Co–P(1)	2.072 (1)	Fe–C(4)	2.068 (6)
Co–P(2)	2.086 (2)	Fe–C(5)	2.062 (6)
Co–C(1)	1.755 (6)	Fe–C(6)	2.100 (6)
Co–C(2)	1.760 (6)	Fe–C(7)	2.109 (5)
Fe–P(3)	2.084 (1)	C(1)–O(1)	1.141 (6)
Fe–P(4)	2.071 (1)	C(2)–O(2)	1.143 (6)
Interbond Angles			
Fe–Co–P(1)	90.23 (5)	Co–Fe–P(3)	86.63 (4)
Fe–Co–P(2)	81.13 (5)	Co–Fe–P(4)	87.13 (5)
Fe–Co–C(1)	171.9 (2)	Co–FeC′[a]	127.7 (1)
Fe–Co–C(2)	79.0 (2)	P(3)–Fe–P(4)	96.35 (6)
P(1)–Co–P(2)	113.99 (6)	P(3)–Fe–C′[a]	123.1 (1)
P(1)–Co–C(1)	97.8 (2)	P(4)–Fe–C′[a]	124.8 (1)
P(1)–Co–C(2)	111.2 (2)	P(1)–N(1)–P(4)	113.72 (2)
P(2)–Co–C(1)	96.3 (2)	P(2)–N(2)–P(3)	109.8 (2)
P(2)–Co–C(2)	130.2 (2)	Co–C(1)–O(1)	177.6 (5)
C(1)–Co–C(2)	97.2 (3)	Co–C(2)–O(2)	174.0 (6)

[a] C′ is the centroid of the cyclopentadienyl ring.

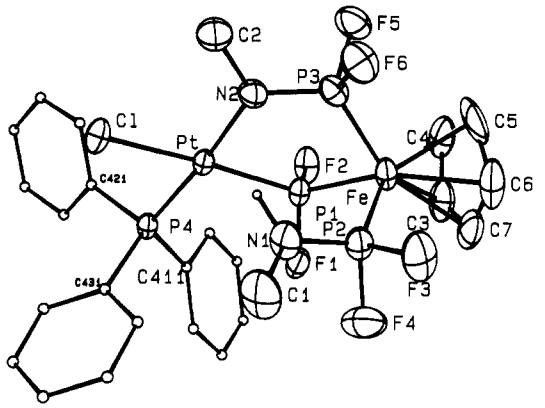

Figure 2. A perspective view of cpFe(PF$_2$NHMe)(μ-PF$_2$)(μ-PF$_2$NMe)PtCl(PPh$_3$) (2). Thermal ellipsoids are drawn at the 50% probability level except for the phenyl carbon atoms and the hydrogen attached to N(1) which are arbitrarily small for clarity. All other hydrogen atoms are omitted.

those in FeCo(CO)$_5$(P(OMe)$_3$)$_2$(μ-PPh$_2$) (2.706 (1) Å)[45] and in FeCo(CO)$_7$(μ-AsMe$_2$) (2.703 (6) Å).[46] Despite its length, the fact that it is intermediate between the two intraligand P–P distances (P(1)–P(4) = 2.775 (2) Å; P(2)–P(3) = 2.717 (2) Å) suggests that it represents an attractive interaction. As with cpFe(μ-MeN(PF$_2$)$_2$)$_2$IrCl$_2$(PMe$_2$Ph)[8] it is not clear whether to consider this interaction as a covalent bond between 17-electron Fe(I) and Co(0) centers or as a donor–acceptor interaction from an 18-electron Co(−1) center to a 16-electron Fe(II) center but given the chemistry associated with the formation of 1, we are inclined to favor the former. The coordination about iron is of the familiar "piano stool" geometry while that about cobalt can best be described as a severely distorted trigonal bipyramid. This distortion involves primarily a displacement of the equatorial ligands toward the iron atom and an opening of the P(2)–Co–C(2) angle from the ideal value of 120°. Despite the displacement of the equatorial carbonyl group toward iron, there is no indication that it participates in any significant semibridging interaction. All other parameters appear normal.

Table VIII. Selected Bond Distances (Å) and Interbond Angles (deg) for cpFe(PF$_2$NHMe)(μ-PF$_2$)(μ-PF$_2$NMe)PtCl(PPh$_3$) (2)

Bond Distances			
Pt–Cl	2.380 (2)	Fe–C(3)	2.06 (1)
Pt–P(1)	2.205 (2)	Fe–C(4)	2.07 (1)
Pt–P(4)	2.246 (2)	Fe–C(5)	2.07 (1)
Pt–N(2)	2.087 (7)	Fe–C(6)	2.10 (1)
Fe–P(1)	2.118 (2)	Fe–C(7)	2.07 (1)
Fe–P(2)	2.094 (3)	P(2)–N(1)	1.589 (8)
Fe–P(3	2.096 (3)	P(3)–N(2)	1.580 (8)
Interbond Angles			
P(1)–Pt–Cl	171.67 (9)	P(2)–Fe–C′[a]	121.6 (5)
P(1)–Pt–P(4)	98.12 (8)	P(3)–Fe–C′[a]	127.5 (5)
P(1)–Pt–N(2)	86.6 (2)	Fe–P(1)–Pt	118.6 (1)
P(4)–Pt–N(2)	175.3 (2)	Fe–P(2)–N(1)	124.3 (3)
P(4)–Pt–Cl	85.08 (2)	Fe–P(3)–N(2)	107.4 (4)
Cl–Pt–N(2)	90.4 (2)	Pt–N(2)–P(3)	120.4 (4)
P(1)–Fe–P(2)	92.9 (1)	Pt–N(2)–C(2)	120.0 (7)
P(1)–Fe–P(3)	86.2 (1)	P(3)–N(2)–C(2)	118.3 (7)
P(1)–Fe–C′[a]	125.0 (5)	P(2)–N(1)–C(1)	124.8 (8)
P(2)–Fe–P(3)	93.4 (1)		

[a] C′ is the centroid of the cyclopentadienyl ring.

(b) cpFe(PF$_2$NHMe)(μ-PF$_2$)(μ-PF$_2$NMe)PtCl(PPh$_3$) (2). A perspective view of **2** and pertinent bond distances and interbond angles appear respectively in Figure 2 and Table VIII. Apart from a relatively short contact of 2.37 Å between F(3) and a cyclopentadienyl hydrogen bound to C(4) of an adjacent molecule there are no unusual intermolecular contacts. The coordination spheres of the Pt and Fe atoms are respectively slightly distorted square planar and "piano stool", respectively. The Pt–Fe separation of 3.717 (1) Å is clearly too long for any direct metal–metal interaction. In a formal sense, **2** can be viewed as a Pt(II) complex of a chelating [cpFe(PF$_2$NHMe)(P̈F$_2$)(PF$_2$N̈Me)]$^-$ ligand. Thus the Pt–N(2) distance of 2.087 (7) Å is within the range previously established for Pt(II)–amide complexes (2.013 (8)–2.09 (2) Å)[60-63] while the Pt–P(1) distance compares well with those

(40) Campbell, I. L. C.; Stephens, F. S. *J. Chem. Soc., Dalton Trans.* **1975**, 22.
(41) Campbell, I. L. C.; Stephens, F. S. *J. Chem. Soc., Dalton Trans.* **1975**, 226.
(42) Grimes, R. N.; Sinn, E.; Maynard, R. B. *Inorg. Chem.* **1980**, *19*, 2384.
(43) Matachek, J. R.; Angelici, R. J.; Schugart, K. A.; Haller, K. J.; Fenske, R. F. *Organometallics* **1984**, *3*, 1038.
(44) Krusic, P. J.; Baker, R. T.; Calabrese, J. C.; Morton, J. R.; Preston, K. F.; Le Page, Y. *J. Am. Chem. Soc.* **1989**, *111*, 1262.
(45) Baker, R. T.; Calabrese, J. C.; Krusic, P. J.; Therien, M. J.; Trogler, W. C. *J. Am. Chem. Soc.* **1988**, *110*, 8392.
(46) Keller, E.; Vahrenkamp, J. *Chem. Ber.* **1976**, *109*, 229.
(47) Grosse, J.; Schmutzler, R.; Sheldrick, W. S. *Acta Crystallogr.* **1974**, *B30*, 1623.
(48) Ling, S. S. M.; Jobe, I. R.; McLennan, A. J.; Manojlović-Muir, L.; Muir, K. W.; Puddephatt, R. J. *J. Chem. Soc., Chem. Commun.* **1985**, 566.
(49) Manojlović-Muir, L.; Muir, K. W. *J. Organomet. Chem.* **1981**, *219*, 129.
(50) Al-Resayes, S. I.; Hitchcock, P. B.; Nixon, J. F. *J. Organomet. Chem.* **1984**, *267*, C13.
(51) Kurasov, S. S.; Eremenko, N. K.; Slovokhotov, Yu. L.; Struchkov, Yu. T. *J. Organomet. Chem.* **1989**, *361*, 405.
(52) Manojlović-Muir, L.; Muir, K. W.; Solomun, T. *J. Organomet. Chem.* **1979**, *179*, 479.
(53) Mingos, D. M. P.; Williams, I. D.; Watson, M. J. *J. Chem. Soc., Dalton Trans.* **1988**, 1509.
(54) Briant, C. E.; Evans, D. G.; Mingos, D. M. P. *J. Chem. Soc., Dalton Trans.* **1986**, 1509.
(55) Bender, R.; Braunstein, P.; Fischer, J.; Ricard, A.; Mitschler, A. *Nouv. J. Chim.* **1981**, *5*, 81.
(56) Hallam, M. F.; Howells, N. G.; Mingos, D. M. R.; Wardle, R. W. M. *J. Chem. Soc., Dalton Trans.* **1985**, 845.
(57) Auburn, M.; Ciriano, M.; Howard, J. A. K.; Murray, M.; Pugh, N. J.; Spencer, J. L.; Stone, F. G. A.; Woodward, P. *J. Chem. Soc., Dalton Trans.* **1980**, 659.
(58) Boag, N. M.; Green, M.; Howard, J. A. K.; Stone, F. G. A.; Wadepohl, H. *J. Chem. Soc., Dalton Trans.* **1981**, 862.
(59) Boag, N. M.; Green, M.; Howard, J. A. K.; Spencer, J. L.; Stansfield, R. F. D.; Thomas, M. D. O.; Stone, F. G. A.; Woodward, P. *J. Chem. Soc., Dalton Trans.* **1980**, 2182.
(60) Sarneski, J. E.; McPhail, A. T.; Onan, K. D. *J. Am. Chem. Soc.* **1977**, *99*, 7376.

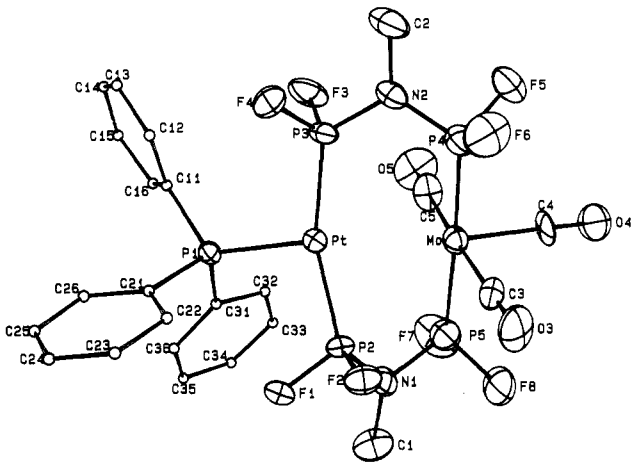

Figure 3. A perspective view of $Pt(PPh_3)(\mu\text{-}PNP)_2Mo(CO)_3$ (4). Thermal ellipsoids are drawn at the 30% probability level except for the phenyl carbon atoms which are arbitrarily small for clarity. Hydrogen atoms are omitted.

to the $MeN(PF_2)_2$ ligands in 8 (Table XI). The P(3)–N(2) and P(2)–N(1) distances are equivalent and significantly shorter than the P–N distances (1.62 (1)–1.69 (1)) for the intact $MeN(PF_2)_2$ ligands in 1, 4, and 8 consistent with the presence of significant N → P π-bonding. Similar distances have been found for the PF_2NMe ligand in $Fe_2(CO)(PF_2NMe)(\mu\text{-}PF_2)(\mu\text{-}MeN(PF_2)_2)_3$ (1.59 (1) Å)[22] and the PF_2NHMe ligand in $Mo_2(CO)_3(PF_2NHMe)(\mu\text{-}Cl)(\mu\text{-}PF_2)(\mu\text{-}MeN(PF_2)_2)_2$ (1.59 (1) Å).[6c] We also note that the angles about N(2) are close to 120° and the {Pt, N(2), C(2), P(3)} moiety is nearly planar.[64] That the nonbridging ligand on iron is correctly formulated as PF_2NHMe rather than as $PF_2{=}NMe$ is indicated by the appearance of a peak in a difference map of height comparable to those for the phenyl hydrogen atoms and in the correct position for a hydrogen atom bound to N(1). As is evident from Figure 4, this ligand is oriented such that the hydrogen atom on N(1) is directed toward the platinum atom, resulting in a Pt–H separation of 2.83 Å. This orientation is most likely determined by a minimization of intramolecular contacts to the PF_2NHMe ligand rather than a significant Pt–H attraction. The Fe–P(2) and Fe–P(3) distances are significantly longer than the Fe–P distances in 1 and $cpFe(\mu\text{-}MeN(PF_2)_2)_2IrCl_2(PMe_2Ph)$ (2.050 (6), 2.047 (4) Å)[8] but are nonetheless significantly shorter than typical Fe–P distances (e.g. 2.21–2.23 Å in $[cpFe(CO)(PPh_3)(C(=CH_2)PPh_3)]BF_4$[65] and $[CpFe(\mu\text{-}CO)(\mu\text{-}CH_3)(\mu\text{-}DPPM)]PF_6$[66]) to non-fluorinated phosphines. We interpret this lengthening as the result of a lowered π-acid character of P(2) and P(3) as compared with the phosphorus atoms of the intact $MeN(PF_2)_2$ ligands because of the enhanced N → P π-bonding.

(c) $Pt(PPh_3)(\mu\text{-}MeN(PF_2)_2)_2Mo(CO)_3$ (4). A perspective view of 4 and pertinent bond distances and interbond angles appear respectively in Figure 3 and Table IX. The closest intermolecular contact is 2.49 Å between O(4) and the hydrogen atom attached to C(23) in an adjacent molecule. The Pt–Mo distance of 2.915 (1) Å is longer than most bonding distances that have been reported previously[67-73] but is within experimental error of that in $[(\eta^5\text{-}C_5H_4Me)Mo(CO)_2(\mu\text{-}DPPM)Pt(DPPM)]_2[Mo_2O_7]$[74] and is slightly shorter than the value of 2.93 Å

Table IX. Selected Bond Distances (Å) and Interbond Angles (deg) for $(Ph_3P)Pt(\mu\text{-}MeN(PF_2)_2)_2Mo(CO)_3$ (4)

Bond Distances			
Pt–Mo	2.915 (1)	Mo–C(3)	2.03 (2)
Pt–P(1)	2.316 (4)	Mo–C(4)	1.99 (2)
Pt–P(2)	2.216 (4)	Mo–C(5)	2.02 (2)
Pt–P(3)	2.206 (4)	C(3)–O(3)	1.13 (2)
Mo–P(4)	2.334 (5)	C(4)–O(4)	1.11 (2)
Mo–P(5)	2.328 (6)	C(5)–O(5)	1.13 (2)
Interbond Angles			
Pt–Mo–P(4)	87.0 (1)	C(3)–Mo–C(5)	177.0 (7)
Pt–Mo–P(5)	89.5 (1)	C(4)–Mo–C(5)	88.5 (8)
Pt–Mo–C(3)	101.6 (5)	Mo–Pt–P(1)	157.1 (1)
Pt–Mo–C(4)	169.6 (7)	Mo–Pt–P(2)	77.0 (1)
Pt–Mo–C(5)	81.4 (5)	Mo–Pt–P(3)	86.2 (1)
P(4)–Mo–P(5)	175.9 (2)	P(1)–Pt–P(2)	97.2 (2)
P(4)–Mo–C(3)	90.1 (5)	P(1)–Pt–P(3)	103.4 (2)
P(4)–Mo–C(4)	91.1 (6)	P(2)–Pt–P(3)	158.6 (2)
P(4)–Mo–C(5)	90.5 (7)	P(2)–N(1)–P(5)	110.4 (8)
P(5)–Mo–C(3)	88.3 (6)	P(3)–N(2)–P(4)	115.8 (8)
P(5)–Mo–C(4)	92.7 (6)	Mo–C(3)–O(3)	175 (2)
P(5)–Mo–C(5)	91.3 (7)	Mo–C(4)–O(4)	179 (2)
C(3)–Mo–C(4)	88.6 (8)	Mo–C(5)–O(5)	177 (2)

Table X. Selected Bond Distances (Å) and Interbond Angles (deg) for $PtCl(P(O)F_2)(PPh_3)_2$ (7)

Bond Distances			
Pt–Cl	2.256 (2)	P(2)–F(1)	1.57 (2)
Pt–P(1)	2.337 (2)	P(2)–F(2)	1.51 (1)
Pt–P(2)	2.264 (2)	P(2)–O	1.50 (1)
Interbond Angles			
P(1)–Pt–P(2)	90.4 (1)	Pt–P(2)–O	114.1 (6)
P(1)–Pt–Cl	92.97 (6)	F(1)–P(2)–O	108.5 (9)
Pt–P(2)–F(1)	114.5 (7)	F(2)–P(2)–O	103.0 (8)
Pt–P(2)–F(2)	109.0 (6)	F(1)–P(2)–F(2)	106.9 (9)

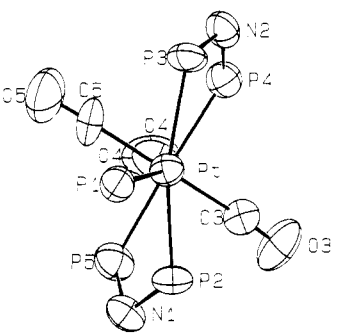

Figure 4. A view of the core of the $Pt(PPh_3)(\mu\text{-}PNP)_2Mo(CO)_3$ molecule (4) along the Pt–Mo axis showing the twist about this axis and the significant distortion from square planar geometry about platinum.

(61) Fryzuk, M. D.; MacNeil, P. A.; Rettig, S. J.; Secco, A. S.; Trotter, J. *Organometallics* **1982**, *1*, 918.
(62) Cooper, M. K.; Downes, J. M.; Goodwin, H. J.; McPartlin, M.; Rosalky, J. M. *Inorg. Chim. Acta* **1983**, *76*, L155.
(63) Eadie, D. T.; Pidcock, A.; Stobart, E. K.; Brennan, E. T.; Cameron, T. S. *Inorg. Chim. Acta* **1982**, *65*, L111.
(64) The crystallographic equation of the weighted least-squares plane is $-6.233X + 11.666Y - 1.618Z + 1.113 = 0$. Distances of the atoms from the plane are as follows: Pt, 0.0000 (3) Å; P(3) −0.003 (2) Å; N(2), 0.082 (8) Å; C(2) −0.077 (12) Å.
(65) Boland-Lussier, B. E.; Churchhill, M. R.; Hughes, R. P.; Rheingold, A. L. *Organometallics* **1982**, *1*, 628.
(66) Dawkins, G. M.; Green, M.; Orpen, A. G.; Stone, F. G. A. *J. Chem. Soc., Chem. Commun.* **1982**, 41.
(67) Bars, O.; Braunstein, P.; Geoffroy, G. L.; Metz, B. *Organometallics* **1986**, *5*, 2021.
(68) Bender, R.; Braunstein, P.; Dusausoy, Y.; Protas, J. *J. Organomet. Chem.* **1979**, *172*, C51.
(69) Braunstein, P.; Keller, E.; Vahrenkamp, H. *J. Organomet. Chem.* **1979**, *165*, 233.
(70) Davies, S. J.; Hill, A. F.; Pilotta, M. U.; Stone, F. G. A. *Polyhedron* **1989**, *8*, 2265.
(71) Powell, J.; Couture, C.; Gregg, M. R.; Sawyer, J. F. *Inorg. Chem.* **1989**, *28*, 3437.
(72) Farr, J. P.; Olmstead, M. M.; Rutherford, N. M.; Wood, F. E.; Balch, A. L. *Organometallics* **1983**, *2*, 1758.
(73) Braunstein, P.; de Meric de Bellefon, C.; Bouaoud, S.-E.; Grandjean, D.; Halet, J. F.; Saillard, J. Y. *J. Am. Chem. Soc.* **1991**, *113*, 5282.

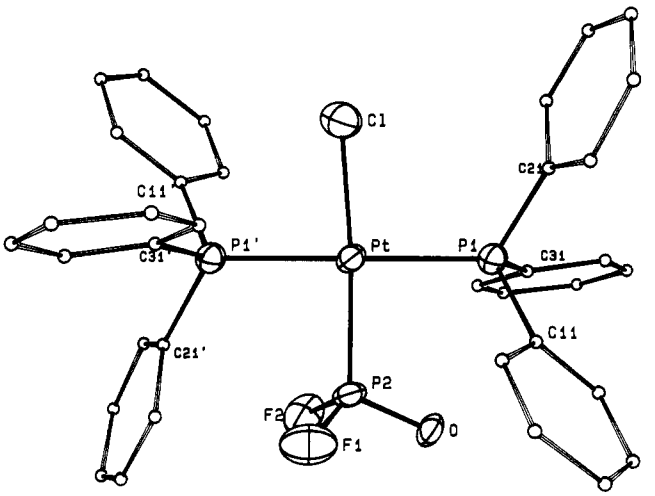

Figure 5. A perspective view of $PtCl(P(O)F_2)(PPh_3)_2$ (7). Thermal ellipsoids are drawn at the 30% probability level except for the phenyl carbon atoms which are arbitrarily small for clarity. Hydrogen atoms are omitted.

proposed earlier for the sum of the covalent radii.[75] As it is significantly longer than the intraligand P–P distances (P(2)–P(5) = 2.724 (7), P(3)–P(4) = 2.789 (6) Å) there is no obvious indication of an attractive interaction, but without it the molybdenum atom would have only a 16-electron count. This is not unprecedented, but as the majority of Mo(0) complexes are 18-electron molecules, we favor the existence of at least a weak Pt → Mo interaction. With this in place, the coordination about Mo is slightly distorted octahedral with the primary distortion being the displacement of the Pt atom away from being collinear with the axial carbonyl ligand (Figure 4). The coordination about Pt is difficult to describe but probably can be considered as severely distorted square planar as is evident from Figure 4. This view also shows a considerable twist about the Pt–Mo axis. There is no obvious reason for this feature but it clearly contributes to the distortion of the coordination sphere of the platinum atom.

(d) $PtCl(P(O)F_2)(PPh_3)_2$ (7). A perspective view of 7 is given in Figure 5 with pertinent bond distances and interbond angles appearing in Table X. No unusual intermolecular contacts occur in the solid state. Considering that the disorder between the Cl and $P(O)F_2$ ligands renders their metrical parameters of limited reliability, all compare well with those reported for the diethylphenylphosphine analog.[47] The disorder also presented problems with identifying the correct position of the oxygen atom of the $P(O)F_2$ ligand and while we consider that this has been done, there remains a possibility that this group is rotationally as well as positionally disordered. Nevertheless the structural study, together with the spectroscopic data confirm the identity of 7.

(e) $Pt_2(\mu\text{-}MeN(PF_2)_2)_3(PPh_3)$ (8). A perspective view of 8 is given in Figure 6 while pertinent bond distances and interbond angles appear in Table XI. The shortest intermolecular contact, 2.33 Å, is between F(32) and a hydrogen atom attached to C(2) of a neighboring molecule. While this is less than the sum of the van der Waal's radii (2.6 Å), there does not appear to be any indication that this represents more than a close packing of molecules. The structure of 8 closely resembles that of $Pt_2(\mu\text{-}dmpm)_3(PPh_3)$ (dmpm = bis(dimethylphosphino)-

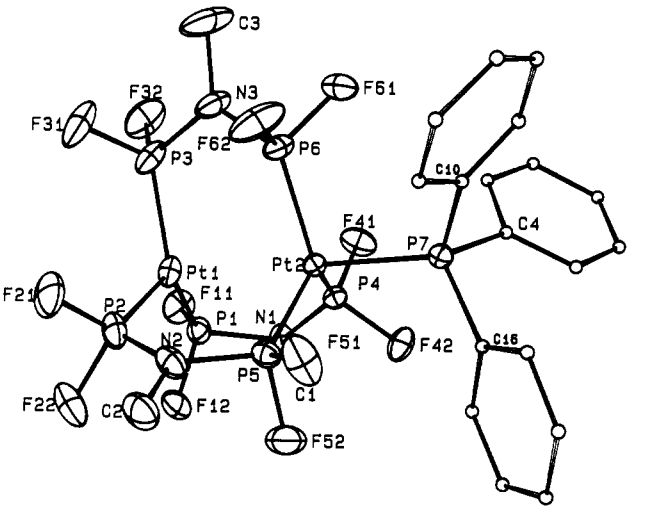

Figure 6. A perspective view of $Pt_2(\mu\text{-}PNP)_3(PPh_3)$ (8). Thermal ellipsoids are drawn at the 30% probability level except for the phenyl carbon atoms which are arbitrarily small for clarity. Hydrogen atoms are omitted.

Table XI. Selected Bond Distances (Å) and Interbond Angles (deg) for $Pt_2(MeN(PF_2)_2)_3(PPh_3)$ (8)

	Bond Distances		
Pt(1)–Pt(2)	2.8911 (4)	Pt(2)–P(4)	2.245 (2)
Pt(1)–P(1)	2.183 (2)	Pt(2)–P(5)	2.252 (2)
Pt(1)–P(2)	2.188 (2)	Pt(2)–P(6)	2.243 (2)
Pt(1)–P(3)	2.189 (2)	Pt(2)–P(7)	2.345 (2)
	Interbond Angles		
Pt(2)–Pt(1)–P(1)	96.85 (5)	P(4)–Pt(2)–P(5)	117.53 (6)
Pt(2)–Pt(1)–P(2)	96.71 (6)	P(4)–Pt(2)–P(6)	118.77 (7)
Pt(2)–Pt(1)–P(3)	97.03 (6)	P(4)–Pt(2)–P(7)	100.59 (6)
P(1)–Pt(1)–P(2)	118.08 (8)	P(5)–Pt(2)–P(6)	115.07 (7)
P(1)–Pt(1)–P(3)	122.95 (8)	P(5)–Pt(2)–P(7)	100.36 (6)
P(2)–Pt(1)–P(3)	114.73 (9)	P(6)–Pt(2)–P(7)	98.63 (6)
Pt(1)–Pt(2)–P(4)	80.02 (4)	P(1)–N(1)–P(4)	116.2 (3)
Pt(1)–Pt(2)–P(5)	80.26 (5)	P(2)–N(2)–P(5)	116.2 (4)
Pt(1)–Pt(2)–P(6)	80.13 (5)	P(3)–N(3)–P(6)	116.3 (4)
Pt(1)–Pt(2)–P(7)	178.76 (4)		

methane)[48] with the significant difference that the Pt(1)–Pt(2) distance is 2.8911 (4) Å in contrast to the clearly nonbonding separation of 3.30 (1) Å in the latter. This Pt(1)–Pt(2) distance is significantly longer than the range generally accepted as representing Pt–Pt bonding interactions (2.611 (2)–2.877 (1))[49-57] but is shorter than those in $Pt_2(COD)_2(\mu\text{-}Me_3SiC{=}CPh)$ (2.914 Å),[58] $(Et_3P)_2Pt(\mu\text{-}PhC{=}CPh)Pt(\mu\text{-}PhC{=}CPh)Pt(PEt_3)_2$ (2.901 (4) Å),[59] and the two longest ones in $Pt_5(\mu\text{-}CO)_5(CO)(PPh_3)_4$ (2.917 (1) and 2.919 (1) Å)[55] where Pt–Pt bonding is considered to be absent or at best questionable. As was seen in $Pt_2(\mu\text{-}dmpm)_3(PPh_3)$, Pt(1) is displaced from the plane of its attached phosphorus atoms *toward* Pt(2) although here the displacement is somewhat greater (0.2613 (3) vs 0.22 Å). Also the coordination geometry about Pt(2) is an even more flattened tetrahedron than in the dmpm complex (Ph_3P–Pt(2)–P = 98.63 (6)–100.59 (6)° vs 101 (1)–107 (1)°) with Pt(2) displaced by 0.3849 (2) Å from the plane defined by P(4)–P(6). These features coupled with the fact that Pt(1) and Pt(2) have 16- and 18-electron configuration, respectively, suggests that a weak Pt(2) → Pt(1) donor interaction may be present. Attempts to further probe this question through a ^{195}Pt NMR experiment were frustrated by the relatively low solubility in suitable solvents. All that could be observed were broad, featureless humps near δ −5500 ppm.

Conclusions. The work reported here indicates that $cpFeCl(PNP)_2$ and $Mo(CO)_3(PNP)_2$ are moderately useful synthons for the directed synthesis of heterobimetallic

(74) Braunstein, P.; de Meric de Bellefon, C.; Lanfranchi, M.; Tiripicchio, A. *Organometallics* **1984**, *3*, 1772.
(75) Bender, R.; Braunstein, P.; Jud, J.-M.; Dusausoy, Y. *Inorg. Chem.* **1984**, *23*, 4489.

complexes. The latter tends to give cleaner reactions since those of the former are complicated by redox processes and ligand reactions.

Acknowledgment. Support by the Petroleum Research Fund under grant 21013-AC3 and the Tulane University Chemistry Department is gratefully acknowledged.

Supplementary Material Available: For 1, 2, 4, 7, and 8, full tables of interatomic distances, interbond angles, calculated hydrogen atom positions, anisotropic thermal parameters, and rms amplitudes of anisotropic displacement (36 pages). Ordering information is given on any current masthead page.

OM920432L

Transition-Metal Derivatives of the Cyclopentadienylphosphine Ligands. 7. Electrochemical Oxidation of $[Rh(\mu\text{-}C_5H_4PPh_2)(CO)]_2$ and Rereduction: An ECE Process Including a Fast Reversible Configurational Switch

Jean-Bernard Tommasino, Dominique de Montauzon, Xiadong He, André Maisonnat, and René Poilblanc*

Laboratoire de Chimie de Coordination du CNRS, UPR 8241 liée par conventions à l'Université Paul Sabatier et à l'Institut National Polytechnique de Toulouse, 205 Route de Narbonne, 31077 Toulouse Cedex, France

Jean-Noel Verpeaux and Christian Amatore*

Ecole Normale Supérieure, Département de Chimie, URA CNRS 1110, 24 Rue Lhomond, 75231 Paris Cedex 05, France

Received June 17, 1992

The electrochemical oxidation of the cyclopentadienylphosphine-bridged complex $[Rh(\mu\text{-}C_5H_4PPh_2)(CO)]_2$ and the reduction of the dicationic parent compound $[Rh(\mu\text{-}C_5H_4PPh_2)(CO)]_2^{2+}$ have been performed at various scan rates from 0.1 to 1200 $V \cdot s^{-1}$ using ultramicroelectrodes. The analysis of the voltammograms and their digital simulation reveal an ECE process where the intervening chemical step is a very fast reversible conformational change ($k_1 = 4000\ s^{-1}$; $k_{-1} = 2000\ s^{-1}$) involving two monocationic intermediates assumed to be respectively a non-metal–metal-bonded mixed-valence complex and a metal–metal-bonded complex (with a bond order closed to 0.5). The high rates of this conformational change, pictured as a disrotatory deformation of the $(\mu\text{-}C_5H_4PPh_2)_2$ central unit, point out to an interesting specificity of this bridging ligand.

Introduction

The hypothesis that two metals kept in close proximity could react cooperatively with substrate molecules has initiated a very broad interest in ligand systems able to lock two metal centers in such a position. As far as the chemistry of low oxidation state transition metals is concerned, tertiary diphosphines have been the most commonly employed ligands; also very short linkages are obtained with four-electron bridging units like for instance the phosphido ($\mu\text{-}PR_2^-$) and the thiolato ($\mu\text{-}SR^-$) anions. The extensive development of the chemistry of metal cyclopentadienyl derivatives and their remarkable properties led us and others to investigate the potentialities, as bridging units, of the heterodifunctional ligands containing a cyclopentadienyl ring,[1a-h] directly linked to a phosphine ligand as in the (diphenylphosphino)cyclopentadienyl anion ($^-C_5H_4PPh_2$) or by a molecular chain as in the (diphenylphosphino)ethylcyclopentadienyl anion ($^-C_5H_4(CH_2)_2PPh_2$). Such ligands are expected to tailor coordination spheres containing both cyclopentadienyl and phosphine ligands either in monometallic chelated species[1h] or in bimetallic bridged species.[1a-g,i] Our recent work on the reactions concerning oxidative addition to the dinuclear ((diphenylphosphino)cyclopentadienyl)rhodium(I) and -iridium(I) complexes $[M^I(\mu\text{-}C_5H_4PPh_2)(CO)]_2$ (M = Rh (1), Ir) has emphasized the quite novel function of the $[\mu\text{-}C_5H_4PR_2]$ bridging unit, working as a "ball and socket joint" between the two molecular moieties.[1i] Thus, this type of flexibility makes the ligand able to accommodate very different metal–metal separations, i.e., from 4.3029 Å in 1 to around 2.7 Å in various types of Rh^{II}–Rh^{II} metal–metal-bonded complexes (2.7796 Å in $[Rh^{II}(\mu\text{-}C_5H_4PPh_2)(\text{pyridine})]_2^{2+}$ (3); 2.7319 Å in $[(COCH_3)Rh^{II}(\mu\text{-}C_5H_4PPh_2)_2Rh^{II}(CO)]^+$ (4); 2.7160 Å in $[(H_3C)Rh^{II}(\mu\text{-}C_5H_4PPh_2)_2Rh^{II}(I)]$ (5)). It has therefore been inferred that the parent dicationic d^7–d^7 complexes $[M^{II}(\mu\text{-}C_5H_4PPh_2)(CO)]_2^{2+}$ (M = Rh (2), Ir) obtained by oxidation of 1 or of the iridium analog, using ferrocenium tetrafluoroborate or silver hexafluorophosphate as oxidizing reagents, offer the same prototypal structure. This was confirmed from the spectroscopic NMR and IR data. In short, the two-electron redox chemically reversible transformation leading from 1 to the dicationic derivative 2

(1) (a) Bullock, M. R.; Casey, C. P. *Acc. Chem. Res.* **1987**, *20*, 167. (b) He, X. D.; Maisonnat, A.; Dahan, F.; Poilblanc, R. *Organometallics* **1987**, *6*, 678–680. (c) Raush, M. D.; Craig Spink, W.; Atwood, J. L.; Baskar, A. J.; Bott, S. G. *Organometallics* **1989**, *8*, 1627–1631. (d) He, X. D.; Maisonnat, A.; Dahan, F.; Poilblanc, R. *Organometallics* **1989**, *8*, 2618–2626. (e) He, X. D.; Maisonnat, A.; Dahan, F.; Poilblanc, R. *J. Chem. Soc., Chem. Commun.* **1990**, 670–671. (f) Anderson, G. K.; Lin, M.; Chiang, M. Y. *Organometallics* **1990**, *9*, 288–289. (g) He, X. D.; Maisonnat, A.; Dahan, F.; Poilblanc, R. *New J. Chem.* **1990**, *14*, 313–315. (h) Kettenbach, R. T.; Butenschön, H. *New J. Chem.* **1990**, *14*, 599–601. (i) He, X. D.; Maisonnat, A.; Dahan, F.; Poilblanc, R. *Organometallics* **1991**, *10*, 2443–2445.

0276-7333/92/2311-4150$03.00/0